NATIONAL INSTITUTE OF ELECTRICITY AND ELECTRONICS
INELEC-BOUMERDES
DEPARTMENT OF RESEARCH

THESIS

Presented in partial fulfillment of the requirement of the

DEGREE OF MAGISTER

In electronic systems engineering

by

Mahfoud CHAFAI

BIOLOGICAL TISSUE CLASSIFICATION AND PATHOLOGY RECOGNITION USING ULTRASONIC A-MODE SIGNAL ANALYSIS.

Defended on june 25 th , 1998 before the jury
-President: Dr A.FARAH (MC - ENP)
-Supervisors: Dr.L.REFOUFI (MC-INELEC)
              Dr. Hadj BOURDOUCEN, MC, INELEC
-Members   Dr. R. R.AKSAS (MC - ENP)
              Dr.M.C.E YAGOUB (MC -USTHB)

Registration number: 03/98

DEDICATION

I dedicate this work to :

My Mother and Father and all my Family

My Wife and Daughters Meriem and Sarah

Cancerous patients suffering from diseases

TABLE OF CONTENTS

CHAPTER 4: ACOUSTICAL IMAGE PROCESSING
FOR PATHOLOGY DETECTION

CHAPTER 5 : A-MODE SIGNAL PROCESSING AND ANALYSIS

-ABSTRACT-

The pulse echo systems are still limited to a qualitative diagnosis, a quantitative analysis based on tissue characterization using A-mode ultrasounds technique is added to improve this diagnosis for early cancer detection.

In this work, B-scan echographic images, obtained from the video output of an echograph using an ultrasonic linear probe, are recorded on a VCR. The recorded still images are introduced into a PC via a video acquisition card to be captured and optimally processed in order to outline the area of interest (AOI). The selected AOI, that includes normal and abnormal region, is converted to gray level matrix and individual column vectors, representing the one-dimensional ultrasonic A-mode signal, are extracted and then analyzed on the base of their amplitude weights to estimate the reflection amplitude and the attenuation coefficient for tissue classification .

The A-mode signal pattern recognition skills play an important role in arriving at reliable diagnosis of inclusions. The obtained A-mode trace is gated into portions corresponding to both consistency and the boundary which are the most used visual clinical features indicative of the pathology. These are expressed in terms of signal diagnostic parameters whose combination is used for further classification of liquid-solid-mixed mass and might be characteristic of the pathology .

However, aspects as acoustic physics, instrumentation and medical interpretation have been covered not only to estimate the acoustic parameters but also to observe the main transformations on the excitation-detected ultrasonic signal for further software correction .

Also, acoustic image processing has been applied, in association with signal processing, to end up with the AOI's and also to determine, preliminary, some textural features which are best analyzed in two-dimensional mode and this will contribute in medical decision making and synthesis.

INTRODUCTION

The pulse-echo system provides a fast, economic, safe and noninvasive examination for anatomic and pathological study of abdominal organs in radiology.

Simultaneously to the development of the other relatively costly imaging techniques CT Scanner, NMR or Aperture radar, spectacular progress in ultrasound imaging has been made in the recent years. The commercial instruments have reached higher performances such as spatial and gray scale resolutions and contrast . Refer to Appendix D .

Since ultrasound diagnosis is currently qualitative, a quantitative approach based on A-mode analysis is added to characterize biological tissue and then improving the accuracy in diagnosis for early cancer detection.

The A-scan technique was developed by Fire stone (1945) to detect the echo producing flaws in the metal. Soon thereafter, French and Al (1950-51) developed 15 MHz pulse-echo system to examine the tumor containing human brains removed post mortem. They noted that the echoes returned by the tumors (confirmed histollogicaly) were larger than those returned by normal tissue. Reid and Wild (1952) used 15 MHz pulse-echo system to examine the human breast tumors, they found that echo amplitudes from cancer were larger than those from the normal tissue [4]. They soon arose a growing desire to obtain cross sectional (tomograms) and to characterize tissues in organs as heart, liver, kidney etc...

The idea of incorporating the capacity for 'tissue characterization' into pulse echo systems came from M. Linzer in 1975 who found that there is wealth of information that could be exploited to diagnose the tissue states [2].

The subject of tissue characterization using ultrasounds has received much more attention nowadays by biomedical engineers community. Most of the investigations published in the literature within the last two decades, from the quantitative approach point of view, are oriented, in majority, to the tissue consistency determination. In connection to this approach,

the statistical and the FFT analysis of the corresponding RF A-mode signal are particularly the mostly used tools [1].

In this work, B-scan image of good quality is obtained and processed to point out the areas of interest from which video A-mode waveforms, contained along acoustic rays, are isolated and studied on the base of their amplitude weights for tissue classification and pathology recognition.

The simultaneous existence of so many different and complex interactions of ultrasounds with biological tissues and their dependence on temperature makes difficulty to isolate anyone of them with a high degree of accuracy. Some necessary simplifying assumptions are made regarding the other interactions that can affect the pulse-echo signal and only backscattering behavior is observed in imaging device with taking into account the attenuation for further time gain compensation (TGC) correction which provides a quite good acquisition .

Therefore, in this study, the parameters estimation approach seeks to estimate the value of a particular acoustical property such as reflection and attenuation coefficients, while structure characterization one is used to investigate in the change in the echostructure of the liver .

The analysis of the reflection coefficient values for selected tissues, in normal or abnormal state, allows the prediction of various imaging results and hence providing different classes of tissue reflectors.

Since the internal architecture of the tissue is stochastic in terms of acoustic scattering properties then, any change in acoustic impedance is expected to occur randomly. Hence, an accurate statistical determination of averages of the A-trace enables a quantitative characterization of a particular biological tissue.

In general, the A-scan signal is considered as a result of a convolution of one dimensional interrogating pulse with some biological tissue. Some processing operations such as an normalization, gating portions of interest and correlation have been done preliminary .

In this case, the A-mode trace is obtained from the envelope detected echo signal which is gated into several portions to end up with traces of interest corresponding not only to the consistency, but also to the boundary feature. This last feature is also important clinically, since it is indicative of the focal decease in the liver [1]. These two clinical features are expressed in terms of A-mode signal parameters whose combination is used firstly, for tissue classification (liquid-solid) and secondly, to characterize the focal pathology for early-warning cancer detection.

This approach has been applied in this case to some liver pathologies, representing respectively benign and malignant cancers, and good quantitative differentiation has been obtained.

The hierarchical main steps for tissue characterization are summarized as ,

```
┌─────────────────────┐
│ Capture acoustic    │
│ image of interest   │
└──────────┬──────────┘
           │
┌──────────┴──────────────┐
│ Optimal image           │         -B scan image Processing
│ processing &Enhancement │
└──────────┬──────────────┘
     ┌─────┴─────────┐
     │ Small & diffuse│
     │ Deases suspection│
     └─────┬─────────┘
   ┌───────┴──────────┐
   │ Outline & selection│
   │ of the Area of Interest│
   └───────┬──────────┘
           │
┌──────────────┐    ┌──────────────────┐
│ 2d Sample    │    │ Amode-line Selection│    -One-dimensional A-mode
│ consistency  │    │ and extraction   │        signal processing
│ analysis     │    └────────┬─────────┘
└──────────────┘             │
              ┌──────────────┴────┐
              │ Amode signal processing│
              └──────────┬─────────┘          Acoustic Data Reference
                         │              ┌────────────────────────┐
              ┌──────────┴─────┐        │ Reflection & Attenuation│
              │ Comparison and │────────│ parameter values       │
              │ Analysis       │        └────────────────────────┘
              └──────────┬─────┘
                         │
              ┌──────────┴──────────┐
              │ Interpretation and  │
              │ Pathology classification│
              └─────────────────────┘
```
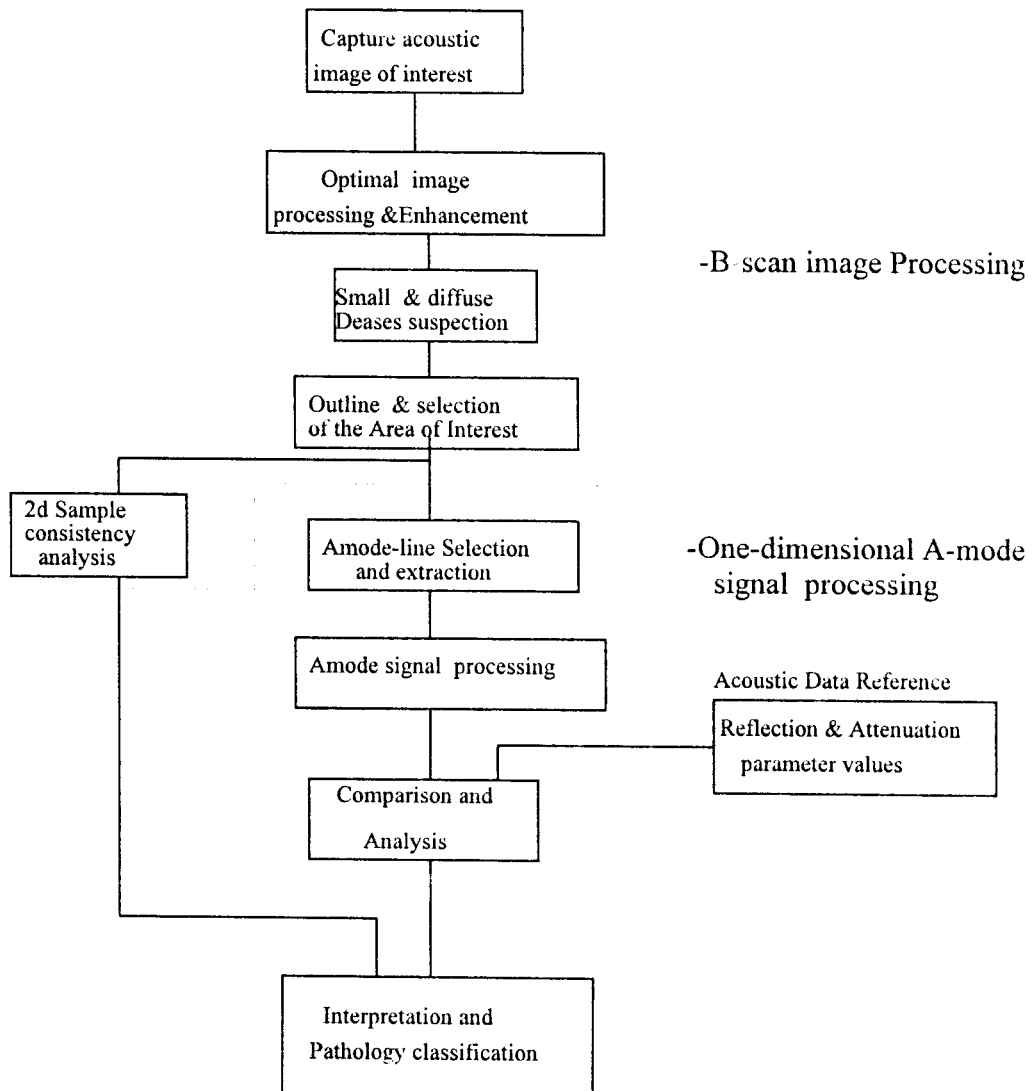
Fig-1.1 Hierarchical steps for tissue characterization

3

In the first chapter is presented an account of the propagation of acoustical waves in the low MHz frequency range and their interaction with biological tissues. The objective of medical ultrasound diagnosis is to use the knowledge of acoustics and the propagation/interaction process to produce acoustical images of tissue and to extract additional information from the image or interaction process that may prove to be clinically relevant . Also, In this chapter a set of acoustical parameter values is collected from different tissues and arranged in the form of classes as data reference for further normalization and analysis.

Chapter two is devoted to the study of the conventional pulse-echo system as well as its more recent version that is used as part of the data acquisition system described in this work. Also described in details , are the electronic signal processing chain and acquisition for further PC software compensation and analysis.
B-scan echographic images, obtained from the video output of an echograph using an ultrasonic linear probe, are recorded on a VCR. The recorded still images are introduced into a PC via a video acquisition card to be captured for further processing and analysis.

Chapter three deals with image processing tasks, suited to acoustic imaging, which are performed to highlight a particular abnormality to the diagnostician in order to point out the suspected pathological or Area Of Interest (AOI) from which data, two-dimensional-samples and column vectors, are extracted and analyzed for pathology detection. Some simple texturale parameters, best analysed in two-dimensions, are also determined to contribute in medical decision making.

In chapter four, the A-mode trace (column vector), obtained from the envelope-detected echo signal, is gated into several portions to end up with traces of interest relevant to both the consistency and the boundary feature. This last feature is also important clinically, since it is indicative of the focal diseases in the liver.
In the boundary analysis, parameters such as the peak value, the thickness, and the nature of the back and front walls are used to identify the type of pathology , whereas the reflection mean amplitude , the periodicity and /or the spatial distribution and the estimated attenuation are used to characterize the consistency of the pathology. The combination of these different signal features is used for tissue classification (liquid-solid) and hence for characterizing the pathology (malignant or benign). A combinational tree diagram, assembling all the previous parameters, has been elaborated for the final diagnostic decision.

ULTRASOUND PHYSICS
AND APPLICATION TO MEDICAL DIAGNOSIS

Today, various aspects of acoustics find application in almost every field of science and engineering ranging from the design of concert halls to medical ultrasonics. It is this later topic that concerns us here, the propagation of acoustical waves in the low MHz frequency range and their interaction with tissue. The objective of medical ultrasound is to use the knowledge of acoustics and the propagation /interaction process to produce acoustical image of tissue and to extract additional information from the image or interaction process that may prove to be clinically relevant. The understanding of the physics of ultrasounds allows a development of new medical ultrasound methods and techniques.

In this chapter a set of acoustical parameters values [1,4,9] is collected from different tissues and arranged in the form of classes as a data reference for further normalization, comparison and analysis.

1-Fundamentals of ultrasonics in biological media

1.1- Introduction to propagation of ultrasonic wave

Ultrasonic waves are longitudinal mechanical waves that can propagates in liquids, solids and gazes.The material particles transmitting such wave oscillate in the direction of the propagation of the wave itself. These oscillations cause alternate compression and raiefaction phenomena in the medium leading to periodic fluctuations of the pressure P around an average value p_o.

The basic linearized wave equation that describes the propagation of the plane wave in an isotropic homogeneous nondissipative fluid [14] is given as :

$$\nabla^2 p = \frac{1}{c^2} \frac{\partial^2 p}{\partial t^2}$$

(2.1)

Where ∇^2 is the three-dimensional Laplacian operator, c the sound velocity, p the pressure at the spatial location (x,y,z) and t the time.

If the coordinate system is chosen so that this plane propagates along the x-axis , (2.1) reduces to,

$$\frac{\partial^2 p}{\partial x^2} = \frac{1}{c^2} \frac{\partial^2 p}{\partial t^2}$$

(2.2)

The general complex form of harmonic solution of this equation for the acoustic incident plane wave can be written,

$$p(x,t) = p_0 . \exp(j(wt - kx))$$

(2.3)

where p_0 is a real constant representing the pressure amplitude, w the angular frequency and k $=w/c$ the wave number. This is an expression for an incident acoustic plane wave propagating in the x direction as a function of time t .

The sourse of this pressure fluctuations is attributed mainly to variations of physical parameters such as the density ρ and the elasticity κ of the considered medium.

1.2- Physical acoustic parameters of biological media

1.2.1- Biological tissue medium

A biological tissue is an extremely complex viscoelastic materiel which has many levels of organization progressing upwards in size from DNA (10 to 10^4 nm) through organelles, cells (10^3 to 10^5 nm), group of cells in connective tissues matrix (10^5 to 10^6 nm) and finally organs (1 to 10 cm) [3].

The biological tissues are classified as: liquid, soft tissue, solid and gas. In the case of the normal liver, which is the organ of interest, it is modeled as a soft tissue, homogeneous isotropic medium.

1.2.2- Medium elasticity

A deformation produced at some point of an elastic medium is transmitted progressively to neighbor points. This mechanism of propagation will use the property of elasticity or compressibility of the tissue medium. This elasticity is characterized by the bulk modulus κ

which is defined as the ratio of change in pressure Δp to the resulting fractional change in the volume $\dfrac{\Delta v}{v}$, hence,

$$\kappa = \frac{-\Delta p}{\Delta v/v} = \frac{-v\Delta p}{\Delta v} \qquad (2.4)$$

1.2.3-Propagation speed

This velocity depends essentially on the bulk modulus of elasticity κ and the density of the medium ρ in the case of gases, liquids and soft tissues :

$$c = \sqrt{\frac{\kappa}{\rho}} \quad \text{m/s} \qquad (2.5)$$

where κ is expressed in $Kg/(m.s^2)$.

In the case of some solids as bones, both longitudinal and shear waves can be propagated and (5) becomes,

$$c = \sqrt{\frac{(\sigma + G)}{\rho}} \qquad (2.6)$$

where σ is Lame's constant and G the modulus of rigidity.

The ultrasonic velocity in soft tissues is almost equal to that in water with a small degree of dispersion (demonstrated in aqueous solution of hemoglobin) [7].The ranges of measured values of the velocity c in the biological tissues and organs are illustrated in figure 2.1, below,
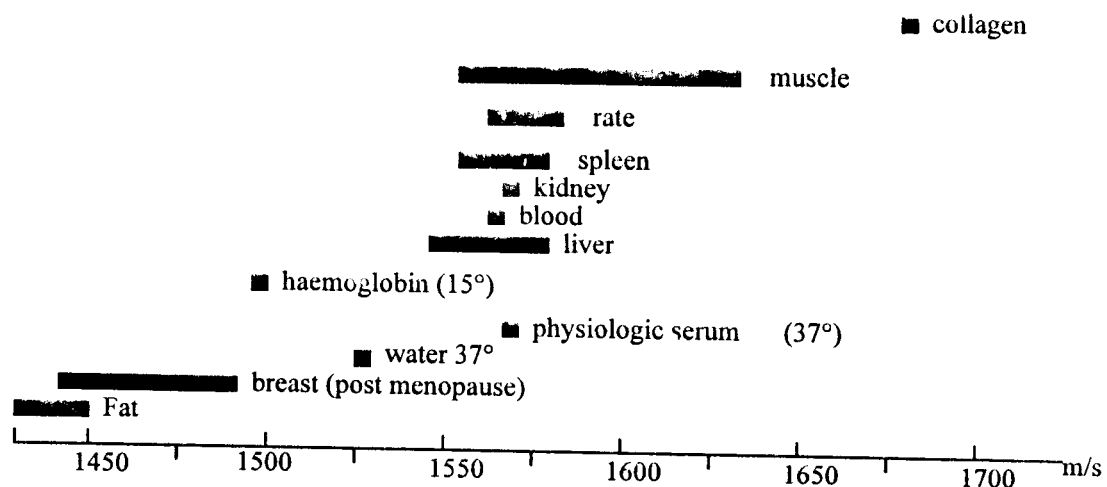

Fig- 2.1 Ultrasonic propagation velocity in biological tissues

1.2.4-The medium density

Eq. (2.5) shows that the density ρ of the tissue medium is also an important parameter. The densities of different tissues and organs are also given in the reference data table 1 in Appendix A. Classification is also established in ascending order from liquid to solid tissue.

1.2.5 -The acoustic impedance

The specific acoustic impedance Z is defined as the ratio of the acoustic pressure p to the particles velocity v:

$$Z = \frac{p}{v} \qquad \text{Kg s}^{-1} \text{ m}^{-2} \tag{2.7}$$

where p and v are distributed values analog to the voltage u and the current i in electricity.

The ratio (p/v) is constant for given tissue and provides one of its acoustic characteristics which depend on its density and velocity c as well as on some parameters related to its elasticity property :

$$Z = \frac{p}{v} = \frac{\rho c v}{v} = \rho c = \sqrt{\rho . \kappa} \tag{2.8}$$

This gives some indication about the tissues strength which is related to bulk modulus κ ; the stiffer the tissue, the higher the wave velocity and the higher the acoustic impedance Z.
An acoustic impedance scale for different tissues, which has been elaborated on the basis of data given in the table 1 of appendix A, is illustrated below in the figure 2.2 .
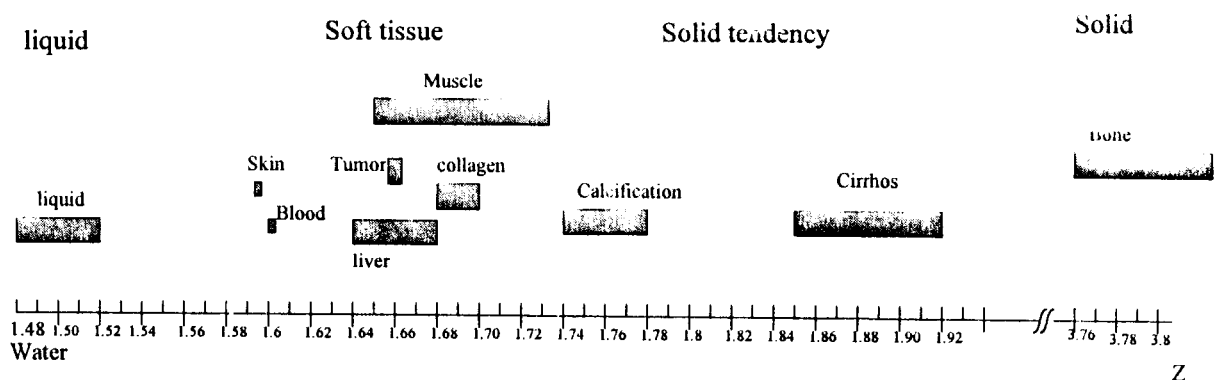

Fig-2.2 Acoustical impedance scale (Kg s^{-1} m^{-2}) for different tissues

1.3- Interaction of ultrasound with biological tissues

When a plane wave encounters an interface between two tissues of different densities and elasticities three processes are fundamentally found : reflection, refraction and attenuation.

1.3.1-Reflection and refraction

When an ultrasonic wave meets an interface between two soft tissue media which differ in characteristic impedance, a proportion of the energy is reflected while the remainder is refracted into the medium beyond the interface as shown in Figure below.

The direction of these waves obeys the same laws of optics [21],

-reflection : $\theta_r = \theta_i$

-transmission : $\dfrac{\sin\theta_i}{\sin\theta_t} = \dfrac{c_1}{c_2}$ (Snell's law)
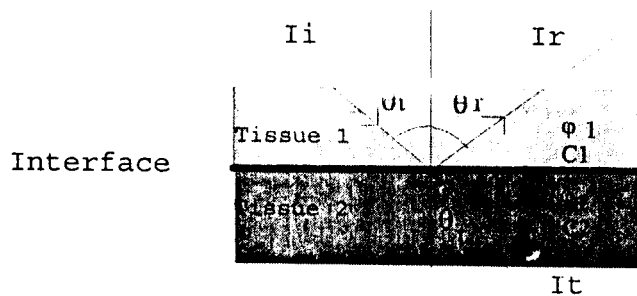

Fig- 2.3 Reflection and refraction at an interface between two different tissues

Where θ_i, θ_r and θ_t are respectively the angles of incidence, reflection and transmission and c_1 and c_2 are the velocities respectively in the media 1 and 2 .

For plane waves at normal incidence the reflection and the transmission coefficients r and t are evaluated as a function of the characteristic acoustic impedances Z_1 and Z_2 of the two adjacent tissues media as follows [21],

$$
\begin{cases}
r = \dfrac{I_r}{I_i} = \left(\dfrac{Z_1 - Z_2}{Z_1 + Z_2}\right)^2 \\[2mm]
t = \dfrac{I_t}{I_i} = \dfrac{4Z_1 Z_2}{(Z_1 + Z_2)^2} \\[2mm]
r + t = 1
\end{cases}
\qquad (2.9)
$$

where I_i, I_r and I_t are respectively incident, reflected and transmitted intensities.

At an oblic incidence θ_i , r is evaluated using the following expression [21],

$$r = \left(\frac{Z_1 \cos\theta_i - Z_2 \cos\theta_t}{Z_1 \cos\theta_i + Z_2 \cos\theta_t} \right)^2 \tag{2.10}$$

This shows that the reflection intensity decreases rapidly as the beam becomes oblic.

In consequence, the echograph will visualize mostly the reflections for which the manipulator has positioned the probe near zero incidence angle and particularly for the zone of interest and hence improving the quality of data acquisition .

The present pulse echo system is based on the envelope detection method and therefore, it is only capable of displaying echo-amplitude information .

Fields and Dunn , considered the classical formula for the amplitude coefficient of backscatterer R [3] as,

$$R = \frac{Z_2 - Z_1}{Z_2 + Z_1} \tag{2.11}$$

The reflected amplitude A_r is directly proportional to the reflection coefficient R ,

$$A_r = A_i . R \tag{2.12}$$

Where A_i is the incident amplitude or pressure.

The larger the difference in the characteristic impedance Z, the larger will be the reflection coefficient R and hence the larger will be the variation of the displayed reflected amplitude. This amplitude is either in phase or out of phase with that of the incident wave[4]. This depends effectively on the specific acoustic impedance value of Z_2 relative to Z_1. If an acoustical incident wave meets an interface where the tissue-medium 2 is of higher impedance than the tissue-medium 1 $(Z_2 > Z_1)$ a positive reflection change is obtained according to equation (2.11) otherwise a negative change is obtained for the reverse case where $Z_2 < Z_1$.

For further convenience, the specific acoustic impedance is normalized with respect to that of water Z_0 as :

$$Z_{nw} = \frac{Z_n}{Z_0} \tag{2.13}$$

Accordingly, if the first medium is water ,the reflection coefficient R becomes,

$$R = \frac{Z_{nw} - 1}{Z_{nw} + 1} \tag{2.14}$$

The refelection amplitude coefficients R is conveniently expressed as a half intensity in dB's,

$$R = 10 Log \left| \frac{Z_{nw} - 1}{Z_{nw} + 1} \right|$$
(2.15)

For computational convenience, the reflection of water is taken as the inferior reference in the gray scale, while the superior limit is that of a perfect reflector. The relative variation of reflected amplitude for two given tissues, in dBs, is estimated as ,

$$\Delta R = A_{r2} - A_{r1}$$
(2.16)

In order to get a positive displayed reflection value, the absolute value of the inferior limit, taken as -25 dBs with respect to the perfect reflector, is added. Hence,

$$A_{r2d} = A_{r2} + 25$$
(2.17)

The analysis of the reflection coefficient values for some selected tissues, in normal or abnormal state, allows the prediction of various imaging results and hence, providing different classes of tissue reflectors.

The calculated values of the amplitude reflection coefficients corresponding to some interfaces in liver organ and its surrounding tissue are illustrated in figure 2.5 . The results are expressed in decibels over the level from water reflector, so that it is easy to compare one reflectivity with another. Therefore, from imaging result of B-scan we can predict the reflection factor values from an interface and then characterizing the two corresponding tissues .

The values indicated in the corresponding table 2 of appendix A apply only to normal incidence on extensive flat boundary. The reflectivity differs for other angles and curved surfaces.
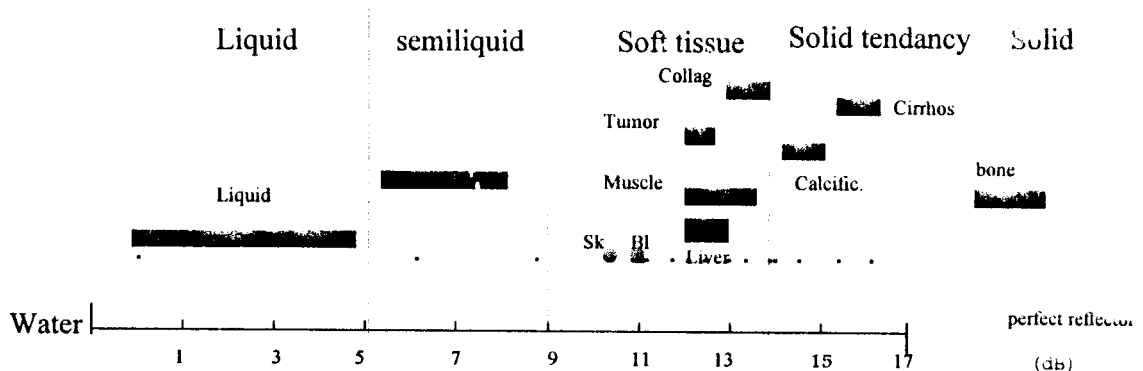
Fig-2.4 Reflection amplitude tissue classes

This graphical reflection scale, shown in figure 2.4, helps in differentiating between different classes of tissue reflections .

Note that several types of liquid exist as hemoglobin, pus and so on .. and that their overall reflection amplitude will depend on the type and the number of the contained particles. In some cases, it could reach that of the soft tissue. However, the empty interval from 5 to 9 dB could be attributed to semiliquid class or mixed class.

The interpretation of the obtained results depends mainly on the amplitude of the reflected components of the ultrasound beam in conjunction with a qualitative estimation of the attenuation.

1.3.2-Attenuation

The intensity of an ultrasonic beam decreases with distance as it propagates in a biological medium. This attenuation is attributed fundamentally to the absorption and the scattering processes.

1.3.2.1-Absorption process

Two types of absorption are generally observed : one is due to the medium viscosity-heat conduction and the other is due to the relaxation process. This later causes most of the overall attenuation

1.3.2.1.1-The classical absorption process

The mechanism of absorption results from the frictional forces associated with the viscosity and heat conduction .

i- Heat conduction

This is a process in which acoustic energy is converted to heat at the site of the interaction. The particles of a homogeneous biological medium can absorb a fraction of an incident energy and then releasing some thermal energy whose rate of increase of the temperature $\frac{\Delta T}{\Delta t}$ is proportional to the ultrasonic intensity I i,e ,

$$\frac{\Delta T}{\Delta t} = K.I \qquad (2.18)$$

ii-Absorption due to the medium viscosity:

The viscosity of the medium opposes the particle motion and so absorption of energy occurs.For a diluted medium this absorption increases wish the square of the applied frequency F. This increase is faster for biological tissues or a concentrated medium. In the case of blood, accurate results have been obtained on account of its homogeneity (Carten..n Schwann). The ratio α/F increases with the frequency in the range 1 to 10 MHz , and the absorption seems to be determined largely by the total protein content [7].

The classical theory of absorption [14] yields an absorption coefficient that is proportional to the square of the frequency , given by :

$$\alpha_c = \frac{(4\pi^2)F^2}{\rho_0 c^2}\left[\frac{4\eta_s}{3} + \frac{(\gamma-1)\chi}{C_p}\right]$$ (2.19)

where α_c denotes absorption due to viscosity and heat conduction, η_s is the coefficient of the shear viscosity, γ the ratio of the specific heats, C_p the heat capacity at constant pressure, χ the thermal conductivity, and ρ_0 the medium density.

1.3.2.1.2-The relaxation absorption process:

Absorption in biological tissues is meanly due to relaxation mechanism [7]. The equilibrium which exists between the various forms of energy is disturbed by the passage of an ultrasonic wave. Because the equilibrium times are not instantaneous, energy phase relationships, which result in absorption, may occur. At low frequency, the phase delay is small and the absorption is constant. The absorption increases with increasing frequency to a limit at which the shared energy is in out of phase. Above this frequency limit, the absorption slope changes because there is less time for energy to flow from one form to another. In another word , at some high frequency, the equilibrium reaction, molecular dissociation-association, cannot be performed in phase with this pressure perturbations and consequently heat will results.

Such processes are also described in terms of relaxation phenomena and an associated relaxation time. For example , the translation motion of the sound wave could have an effect on the vibrational or rotational structure of the fluid such that at a certain frequency structural rearrangements could occur fueled by the energy of the sound wave and causing an effective increase in absorption as shown in the Fig- 2.5.
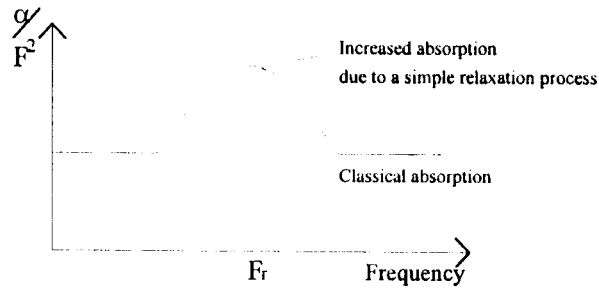
Fig-2.5 Increased absorption due to a single relaxation peak at the frequency Fr

As the structural complexity of the fluid increases, the number of relaxation processes required to describe the absorption of sound also increases.

The absorption coefficient α_R for a collection of relaxation processes is most conveniently written as the sum [14],

$$\alpha_R = F^2 \sum_{i=1}^{n} \frac{C_i}{1 + \left(\dfrac{F}{F_{R_i}}\right)^2} \tag{2.20}$$

where C_i is a descriptive constant or function associated with the ith process.

In general, relaxation processes not only raise the magnitude of the absorption over its classical value but also change the frequency dependence as shown in the figure2.3. As the number of relaxation processes increases, the absorption coefficient goes from $\alpha_r \sim F^2$ to $\alpha_r \sim F$. In fact, it can be shown that as the number of the processes becomes infinite ($n \to \infty$) in eq. (2.20) the frequency dependence of α goes to unity. This analysis is still under experimentation : complex solution of macromolecules as well as tissues have absorption coefficients that have near-unity dependence on frequency[14].

Therefore, the total absorption coefficient is given by ,

$$\mu = \alpha_v + \alpha_R \tag{2.21}$$

The coefficient μ, which depends also on the propagation medium, is conveniently expressed as function frequency F,ie, [6]

$$\mu = \mu_0 F^{\beta} \tag{2.22}$$

with $1 < \beta < 2$ for soft tissues.

In the low frequency range 1 to 3.5 Mhz, the attenuation coefficient in the soft tissue is slightly proportional to frequency ($\beta \approx 1.1$) and then could be approximated as,

$$\mu = \mu_0 F \tag{2.23}$$

1.3.2.1.3-The absorption law

In homogeneous media, the amplitude a of an acoustic wave decreases exponentially with distance x from the source as,

$$p = p_0 e^{-\mu x} \tag{2.24}$$

where p_0 is the vibration pressure amplitude at the source.

The transmitted ultrasonic intensity is given by,

$$I_t = I_0 e^{-2\mu x} \tag{2.25}$$

The attenuation A_e of an ultrasonic wave is determined using decimal logarithm of the intensities ratio, hence

$$A = 2.3\log(\frac{I_0}{I_t})^{1/2} = \mu x \Leftrightarrow A_t = (\frac{2}{2.3}\mu)x \tag{2.26}$$

Making use of equ. (2.26) A_t becomes,

$$A_t = (\frac{2}{2.3}\mu_0 F)x = \alpha.x.F \tag{2.27}$$

α is conveniently expressed in term of coefficient per unit length and frequency as,

$$\alpha = \frac{A_t}{cmMhz} \tag{2.28}$$

However, blood attenuates the ultrasound the least, followed by the fat, brain, kidney, liver, muscle, bone and lung as shown in figure 2.6. The attenuations in both bone and lung are much greater and hence ultrasounds are largely confined to the soft tissues which are not obscured by bone or gas.
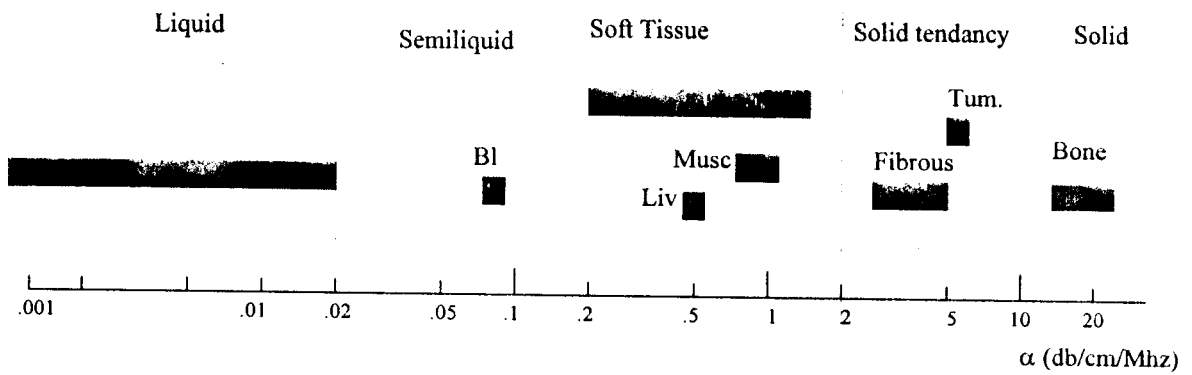
Fig-2.6 Amplitude Attenuation coefficients

In the case of several successive tissue media 1,2,3..n with respective attenuations $A_{t1}, A_{t2}... A_{tn}$ the total attenuation can be expressed by the following expression,

$$A_{tt} = \sum_1^n A_{ti} = \sum_1^n \alpha_i x_i F \qquad (2.29)$$

1.3.2.2-Scattering processes

This is due to the direction change from the mean path of the radiated energy of the beam. A particle, that is considered as an elastic sphere, interacts with an acoustic beam in different ways depending on the relative value of its radius r_d to the wavelength λ of the beam [12] .

1.3.2.2.1- Reflection and refraction : case where $\lambda << r_d$

If the wavelength of the incident radiation is much less than the dimension of the scattering particle or interface, specular reflections occur and the amount of the reduced intensity is given as [12]:

$$\Delta I_r = \sum R_i I_i \qquad (2.30)$$

But this reflectivity depends also on the form and the nature of the wall at the interface. If the interface is smooth and plane a simple reflection takes place with higher intensity at specular condition. At the other extreme, if the interface is rough and curved, a part of the beam reaching the curved zone may be reflected with weak intensity and out of the direction of the detecting field of the probe as shown in Fig 2.7a ; while the part reaching the rough region, that is composed of asperities, behaves as a diffusing region in arbitrary direction and towards the probe. Then the resulting detected wave will be a mixture of reflected and diffused waves from the obstacle as illustrated below, in the figure 2.7-c.

Probe   Probe

detecting field

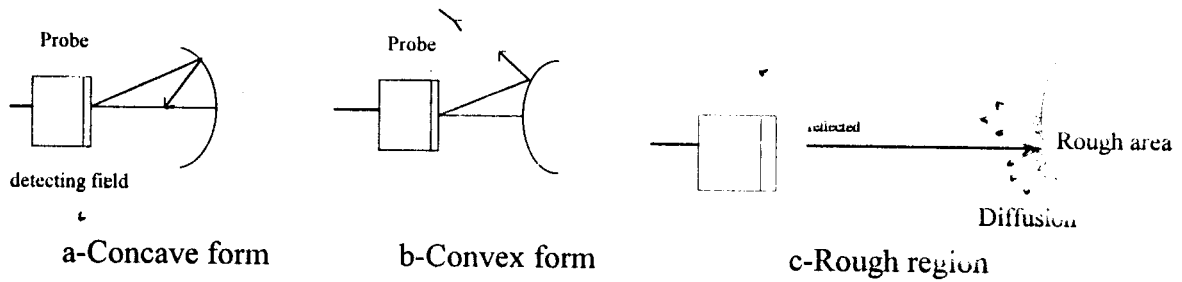a-Concave form   b-Convex form   c-Rough region

Fig-2.7 Reflection in the curved and rough regions

Note that in case of interaction of ultrasounds with solid as bone, energy mode conversion takes place and hence the incident longitudinal wave produces also shear waves causing energy reduction.

1.3.2.2.2-*Diffusion : case where* $\lambda >> r_d$

If the particle, exhibiting the variation, is small compared to wavelength of the incident beam, scattering is of Rayleigh type and then tends to be isotropic. The particle contracts and dilates at a constant speed following the pressure variation and it behaves as a secondary source that reradiates a small fraction of the acoustic energy in all directions in space with the same frequency as the incident wave as shown in figure 2.7-c.

The intensity of the diffused wave, following one direction β with respect to that of the beam, is inversely proportional to the fourth power of the wavelength and it is given by the Rayleigh law [ ],

$$I_d = \frac{I_0 f(\beta) R^6}{\lambda^4}$$

(2.31)

This expression indicates that at the given direction β the diffusion intensity decreases faster when the wavelength increases with respect to the size of particle. For some directions, in which the diffused rays are out of the probe detecting field, the intensity reduction is then,

$$\Delta I_{dif} = \sum I_{di}$$

(2.32)

1.3.2.2.3-*Complex scattering : case* $\lambda = r_d$

For an incident wave with a wavelength of the same magnitude as the dimension of the scatterer, the scattered waves form a very complex patterns composed of reflection, refraction and diffusion waves [12].

For an ultrasonic transducer of $2a$ diameter and wavelength λ, the width of an ultrasonic beam remains constant for a distance $D = a^2 / \lambda$ and start diverging by an angle given as follows [21],
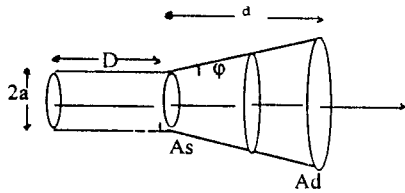
$$\varphi = \sin^{-1} (0.61 \lambda / a) \qquad (2.33)$$

Fig 2.8 Beam divergence

At distance d far from the limit of the Franhofer distance D, the intensity becomes,

$$I_d = I_s \frac{A_s}{A_d} = I_s \frac{\pi a^2}{\pi (a + d \tan \varphi)^2} < I_s \qquad (2.34)$$

where A_s and A_d are the radiated areas respectively at D and $D+d$; I_s and I_{xd} denote intensities respectively at source and at the distance d from the Franhofer limit.

In this case the energy becomes spread out over larger areas and then the energy per unit area or the intensity I_{xd} decreases. The intensity reduction is then:

$$\Delta I_{div} = I_s - I_{xd} \qquad (2.35)$$

1.3.2.3-The total attenuation

The overall attenuation may be presented by the following attenuation tree in figure below,
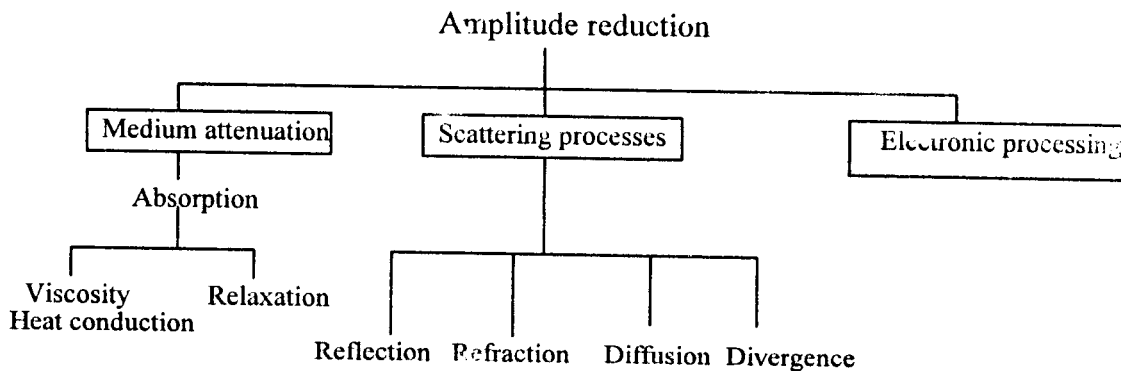

Fig-2.9 Attenuation causes Tree

The overall amplitude reduction is written as,

$$A_{iT} = \Delta I_{ab} + (\Delta I_R + \Delta I_{dif} + \Delta I_{div}) + \Delta I_{inst.} \qquad (2.36)$$

Since most of the attenuation occurs in absorption and reflection, the previous equation simplifies to,

$$A_{iT} = \Delta I_{ab} + \Delta I_R = \sum_1^n \alpha_i x_i F + \sum R_i I_i \qquad (2.37)$$

Note that the amplitude attenuation, that may be caused by the electronic processing circuit as well as the transducer, is not considered in this case.

The estimation of the attenuation parameter helps in getting the time gain compensation (TGC) setting as correct as possible for a specified organ or portion of it allowing better quality of acquisition for further reflection amplitude analysis.

2- Reflection amplitude and attenuation coefficient estimation

The simultaneous existence of so many different and complex interactions of ultrasounds with biological tissues and their dependence on temperature makes difficult to isolate anyone of them with a high degree of accuracy. Some necessary simplifying assumptions are made regarding the other interactions that can affect the pulse-echo signal and only backscattering behavior is observed in imaging devices when taking into account the attenuation estimation for tissue characterization [2].

2.1-Estimation of the reflection amplitude

Note that, the small difference in acoustic impedance between biological tissues is such that the echo sent back by their interfaces is easily detected by the pulse echo system, while the major part of the incident ultrasound wave is transmitted and used for further exploration of the examined organ with fairly large depth ranges.

In this study, we have considered only the first order reflections with planar interfaces, in which the ultrasound beam can either be specularly reflected or backscattered with taking into account its progressive attenuation with distance in accordance with the proposed model for the amplitude reduction.

If the tissue is modeled as an n-layers medium to be traversed by an ultrasound beam, the detected reflected amplitude at the K^{ih} interface can be expressed as follows ,

$$\frac{Ar_{k,k+1}}{A_{R12}} = \frac{A_i\left(\prod_{p=2}^{p=k}(1 - R^2_{p-1,p})\right)\exp(-2\sum_{m=1}^{m=k-1}\alpha_m x_m).\exp(2\alpha_c.X).R_{k,k+1}}{A_i R_{12}}$$

$$= \left(\prod_{p=2}^{p=k}(1 - R^2_{p-1,p})\right)\exp(-2\sum_{m=1}^{m=k-1}\alpha_m.x_m + 2\alpha_c X) \tag{2.41}$$

Taking the logarithm of both sides of equation (2.41) and expressing the new quantities in dBs, the previous equation becomes,

$$ArL_{k,k+1} - AL_{R12} = \sum_{p=2}^{p=k} Log(1 - R^2_{p-1,p}) + \frac{2}{2.3}(\alpha_c X - \sum_{m=1}^{m=k+1}\alpha_m.x_m) \tag{2.42}$$

If each layer of the considered medium presents the same attenuation coefficient α_m ,then the overall attenuation α_T becomes,

$$\alpha_T = \sum_{m=1}^{m=K+1}\alpha_m.x_m = \alpha_m.X \tag{2.43}$$

Therefore, the attenuation coefficient at the working frequency of 3.5 MHz per cm is evaluated as,

$$\alpha_T \cong \alpha_c - \frac{(ArL_{k,k+1} - AL_{R12}) - \sum_{p=2}^{p=K} Log(1 - R^2_{p-1,p})}{X} \tag{2.44}$$

Finally the attenuation at 1 MHz per cm is then estimated to be,

$$\alpha_p = \frac{\alpha_T}{F} = \frac{\alpha_T}{3.5} \tag{2.45}$$

Note that in the case of tissue with solid tendency consistency inside the liver, the amplitude reduction due to shear waves is relatively small and then can be neglected.

$$Ar_{k,k+1} = \begin{cases} A_i R_{12} & \text{for } k = 1 \\ A_i \left(\prod_{p=2}^{p=k}\left(1 - R_{p-1,p}^2\right) \right) \exp\left(-2 \sum_{m=1}^{m=k-1} \alpha_m x_m \right). R_{k,k+1} & \text{elsewhere} \end{cases} \tag{2.38}$$
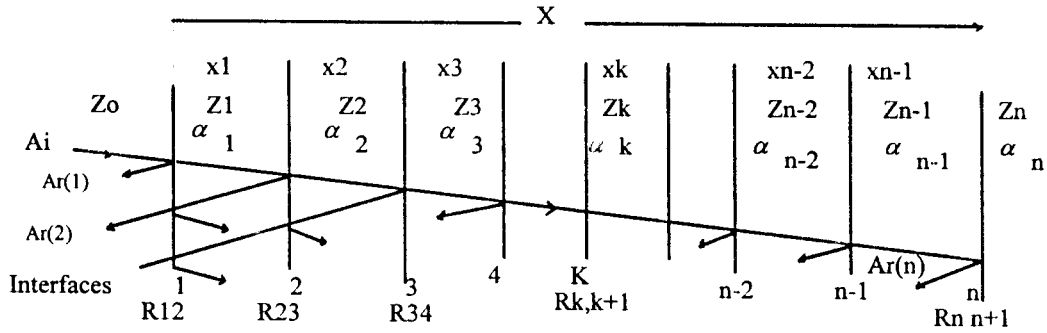

Fig-2.10 Reflections at different interfaces of an n-layer tissue

Where n is the number of interfaces and Z_k, α_k and x_k are respectively, the specific acoustic impedance, the attenuation coefficient and the thickness of the Kth layer.

The overall detected A-trace for the n-layer tissue is evaluated as ,

$$A_r(n) = A_i R_{12} + A_i \sum_{k=2}^{k=n}\left(\prod_{p=2}^{p=k}\left(1 - R_{p-1,p}^2\right)\right) \exp\left(-2 \sum_{m=1}^{m=k-1} \alpha_m x_m \right). R_{k,k+1} \tag{2.39}$$

This signal should be applied to a time gain compensation circuit (TGC) in the pulse-echo system to compensate for the attenuation. Since, the TGC function is generally taken as an increasing exponential time function [1] the previous equation becomes,

$$A_c(n) = A_i R_{12} + A_i \sum_{k=2}^{k=n}\left(\prod_{p=2}^{p=k}\left(1 - R_{p-1,p}^2\right)\right) \exp\left(-2 \sum_{m=1}^{m=k-1} \alpha_m x_m \right).\exp(2\alpha_c.X). R_{k,k+1} \tag{2.40}$$

2.2-Estimation of the attenuation in reflection mode

The reflection amplitude reduction at the kth interface is evaluated as the difference between the reflection amplitudes of the front wall A_{R12} and the back wall $Ar_{k,k+1}$ of the inclusion of study. Assuming that both walls are of the same nature and therefore have the same backscattering coefficient $R_{k,k+1}$, the ratio of these amplitudes is expressed as ,

3-The liver echostructure

The liver organ and other constituents of the body are made of tissues that vary widely in structure. The ultrasound beam interacts in different ways at all levels of organization depending upon acoustic properties of the examined tissue. The most important factors involved are the internal anatomy of the organ as shown in figure 2.9, its overall geometry and the intrinsic property of the tissue itself . Refer to Appendix A for acoustic parameters values.
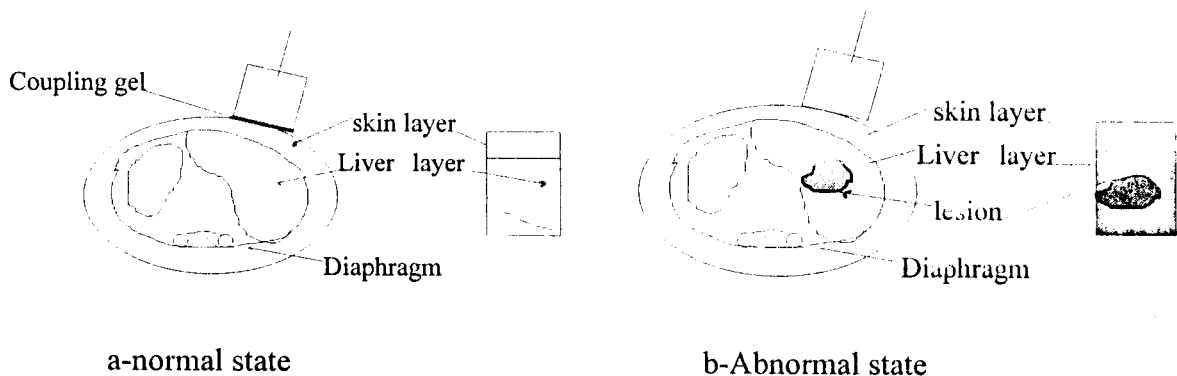

| a-normal state | b-Abnormal state |

FIG.2.11 Anatomic cross-section of the liver

3.1- Liver normal state

The liver has a filled homogeneous echostructure with regular edges and some heterogeneities which are due to vascular sections[18]. The acoustic beam must cross the skin layer and the diaphragm interface in order to reach the liver organ as shown in Fig-2.11 .

The echoes arising from and within the liver organ are the result of a convolution of the interference pattern due to the array of point scatterers constituting the parenchyma of the organ with the shape of the interrogating beam.

However, the liver tissue has a well developed collagen framework which yields a medium echoes intensity . Collagen is extremely well distributed in liver tissues, and is responsible for maintaining both the external and the internal structure of the organ and thus, it is expected to be an important site of echo formation in normal liver tissues [8]. Note that a small proportion of the fat tissue is also contained in the liver.

In some anatomical sections, the surrounding organs such as the kidney and the spleen may be considered for an anatomical mapping and overview for further clinical pattern recognition.

3.2-Liver pathological state

Since this abnormal state, in a limited or a diffused region as shown in figure 2.11-b, may come from a rearrangement in the structure and a change in acoustic properties , the pathological mass causes effectively an ultrasonic interaction different from that of the normal region of the liver. For instance, the liver focal decease's appear as local disruption of parenchymal architecture while the diffuse ones are marked by a general alteration of the parenchymal pattern.

Note that Collagen has also a particular significance in pathological conditions since many inflammatory processes are accompanied by an increase in collagen content of an organ ,whereas tumors may either replace the collagen in the normal tissue or an adjacent fibrous reaction[3].

Some pathological mass,clinically termed as solid, have just tendency to be solid since their acoustic parameters are much less than that of a real solid such as bone or stones etc.

INSTRUMENTATION

1-Pulse-echo system

Any improvement in the pulse echo system requires a good study and a knowledge of the conventional system and its electronics signal processing chain for further PC software correction or compensation and analysis.

Pulse-echo system for ultrasound diagnosis is based on measuring techniques similar to those used in radar. Three modes (or scans) are generally used in medicine: A-scan, B-scan and M-mode. The main interest has been done on the two first modes .

1.1-Principle of A and B modes

1.1.1-A-scan system

When a signal is emitted from an ultrasonic transducer, it is reflected at various discontinuities back to it. The detected echo information is used to drive the vertical deflection plates of the CRT and provides us with the reflected acoustic energy and the depth d of any reflecting interface in tissue where the range of the time of flight t is calculated as ,

$$t = \frac{2d}{c} \tag{3.1}$$

It is one dimensional amplitude versus depth display system that provides one line of exploration. For more details refer to figure 1 of Appendix B.

1.1.2-B-Scan system

This is a two-dimensional system in which a cross sectional image of the scanned region, that is in plane parallel to the direction of the beam, is built up gradually and mapped on the CRT storage system as the probe is moving laterally under specular condition of reflection.

It is fundamentally based on the information provided by a set of echoes in A-scan that are used to modulate the intensity of the CRT electron beam instead of deflecting it vertically.

For a given position of the transducer, the exploration line is represented on the screen by series of dots whose brightness depends on the echo amplitude and whose position in the vertical axis is corresponding to that of a reflecting element in the explored plane.

1.2-The recent pulse-echo system

The pulse-echo system, we have used, consists essentially of an ultrasonic linear array probe, a receiver and a scan-converter with a microcontroller as shown in the Fig-3. 1.
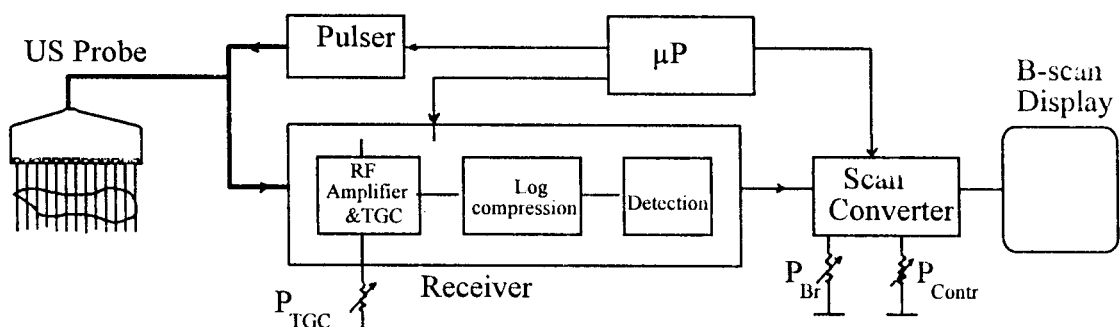

Fig-3.1 The recent pulse echo system

The pulser excites an ultrasonic probe with a high voltage pulse that produces an acoustic wavelet that will be transmitted into a human tissue acting as reflector. The reflected acoustic wave is detected by the same probe, amplified by an RF amplifier to which is associated a TGC circuit, compressed and then demodulated. The obtained envelope detected signal is then displayed on the screen as echo-amplitude information [3] through a digital scan converter as shown in figure 3.1.

For detailed bloc diagram and technical characteristics of the used echograph, refer to figure 4 of Appendix B.

1.2.1-The ultrasonic pulser probe

1.2.1.1-The pulse generator

The excitation is obtained by either short pulse duration of high amplitude (50 to 200 V) or by short train of pulses of frequency F and separated in time causing forcing oscillations.

The choice of the resonant frequencies such as 3.5 MHz or 5MHz results from a compromise between the resolution and the attenuation. High frequencies (>5 MHz) improve the resolution but don't allow a deeper exploration.

In examining the abdomen, the maximum penetration depth is around 20 cm and this corresponds to the pulse-echo acquisition time of 256 μs. Accordingly, this time interval is required to avoid the interference of the returning echo with the transmitted pulse. Therefore the pulse repetition frequency (PRF) must be sufficiently low (< 4000/s) to avoid the pulse-to-pulse ambiguities.

1.2.1.2-The ultrasonic transducer:

When a piezoelectric transducer is pulsed with a voltage pulse profile, an acoustic wavelet starts traveling from each of its faces. In this case, a longitudinal acoustic wave is produced perpendicular to the electrode plates as shown in Fig -3.2.a .

a- Excitation- response   b-Transducer conversion
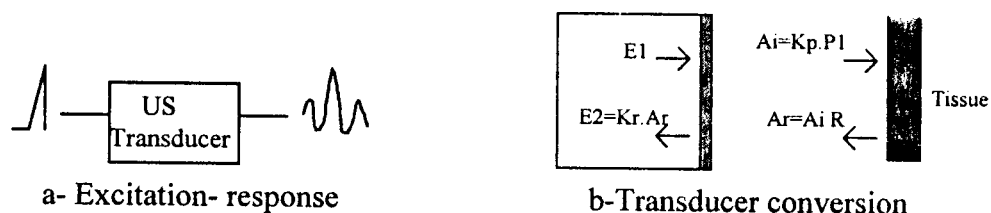
Fig-3.2 Ultrasonic transducer excitation-response

The crystal thickness is equal to half wavelength or odd multiples such that at resonance its mechanical energy is maximum at the emission and the reception modes.

But instead of using a sharply tuned transducer that will respond only near the resonant frequency, it is better to use a broad band, obtained by using short pulses emission, to get more detailed information on tissue material in the form of power spectrum. For abdominal application, transducers with center frequencies of 3.5 and 5 MHz are generally used and a bandwidth of 60% to 100% are typical [14].

However the actual scattering at particular point within the tissue gives rise to a measured electrical signal E that is proportional to the detected pressure Pr. This signal is then processed and applied to the CRT display.

Assuming that the transducer response is linear, the obtained electrical signal is given by:

$$E = K_r . P_r \qquad (3.2)$$

where P_r is the reflected pressure and K_r is the transducer coefficient.

1.2.1.3-The linear array probe

An array of fixed transducers, placed in a linear configuration, are switched sequentially to scan a rectangular cross sectional plane to form a two dimensional image in short time. Such system, based on the A-scans has been developed by Bar and AL in 1971 [].
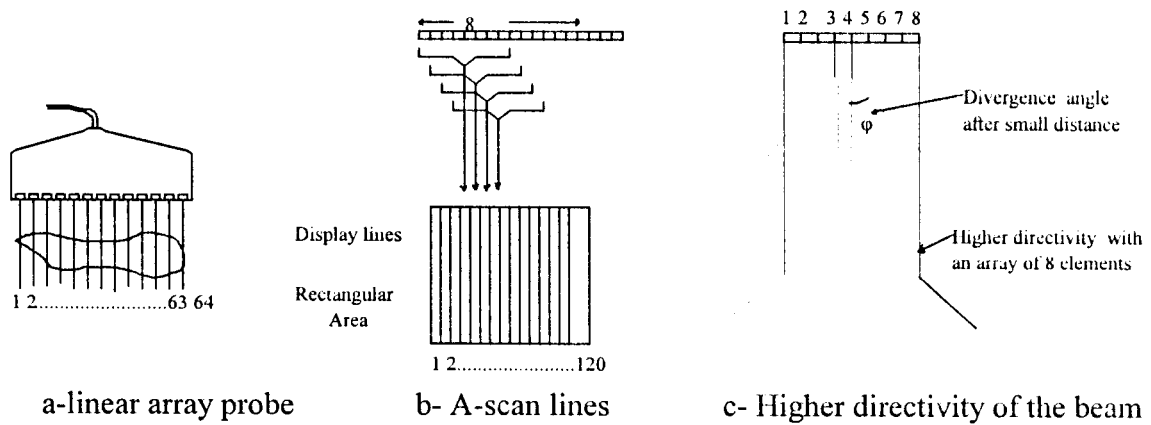

| a-linear array probe | b- A-scan lines | c- Higher directivity of the beam |

Fig-3.3 Linear ultrasonic probe

Note that the used probe is made of an array of *64* fixed transducers, as shown in Fig-3.3a, providing *120* A-scan lines which built up, in real time, a quite good quality B-scan image.
In this case, each line is produced by an array of 8 elements which are stepped along one element at a time leading to a higher directivity as shown in FIG 3.3 c.
The focusing control is provided to allow the examination of any specific small region by using suitable delay lines.

1.2.1.4- Spatial Resolution

The fundamental limitation to the axial resolution of the acoustic imaging system is set by the wavelength λ of the radiation used to examine the tissue. Ultrasound pulse of frequency 2 to 5 MHz traveling at a velocity of 1540m/s has wavelength in the range 1 to 0.3 mm. This is very desirable for visualizing the biological structure of small size in an organ, since this can produce a Rayleigh reflection when it is greater than 1mm and then enough number of data points can be collected for further analysis.

column-pixel number	Bandwidth(max) MHz	pixels/cm	Time of flight (μs)
256	1	12.5	13
512	2	25	13

Table 3.1 Axial resolution values

The transmit-receive cycle is incremented by one transducer after each pulse-echo sequence to generate 120 independent scan lines. Each line is shifted half element to enhance lateral resolution. The multiplexers, inserted in the probe, switch the elements to produce 50 or 60 images per second.

1.2.2-The ultrasonic receiver:

The amplitude of the smallest signal of interest received from within the patient is around 10 μv, and the dynamic range of echoes, equals to that of a tissue impedance variation, extends to about 100 db's.

The reflected acoustic wave is detected by the same probe, amplified by an RF amplifier associated to a TGC circuit which compensates for the attenuation. This RF amplifier is broadly tuned by an LCR network such that its bandwidth covers the center frequency of the ultrasonic emission.

A logarithmic compression is applied to RF output signal whose dynamic range is in the order of 100 db's, because only 50 to 60 db range is required for further screen display. The echo amplitude range is selected following the importance and the density of the clinical information [7].

In practice a full wave demodulation is used when operating in short pulses. This is followed by a low pass filter ,with a cut off frequency less than 3 MHz, which filters out the non-desirable carrier frequency and detects the envelope of the echo signal. A variable control is associated to this detector to provide a suppression of echoes smaller than any chosen level refered generally to noise.

The pulse echo system can be described as an operator within a transfer function H,

$$S(t)=H [A(t)]$$

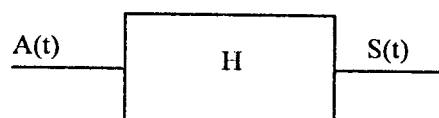<div align="right">(3.3)</div>

A(t) ——— | H | ——— S(t)

Fig-3. 4 Pulse echo system transfer function

Since this system is not always linear, the knowledge of the electronic processing of the signal with the associated user controls at different stages should allow further software correction and compensation to end up with a displayed signal that reflects the original detected signal .

The various electronic processings are summarized in the following table:

Signal waveform	Processing circuit	Response of processing Domain		Output function	U.G.C
		Time	Frequency		
	Transducer			$Vo=Kr.Pr$	
	RF Amplification			$Vo=A.Vi$	
	RF Amplific. with TGC			$V_0 = V_i e^{+\alpha t}$	*
	Full wave rectification			$V_0 = \begin{cases} Vi \ for \ Vi>0 \\ -Vi \ for \ Vi<0 \end{cases}$	
	Rectificat. & envelope detection			$V_o = \dfrac{1}{RC} \int V_{in} .dt$	
	Logarithmic compression			$V_0 = V_a Log(\dfrac{Vi}{C})$	
	Contrast Gain			$V_o = A_c . V_i$	*
	Brightness (dc shift)			$V_0 = V_i + b$	*

Table 3.2 Mean electronic processing options of the pulse echo receiver
    UGC stands for user gain control

1.2.3-Digital scan converter

The demodulated echo signal is then converted by an analog to digital converter (ADC) within minimum word rate of 6 MHz according to Shannon Theorem, stored in the memory to be processed , and then displayed on a TV display using high speed wide dynamic digital to analogue converter (DAC).

The resolution of both ADC and DAC lies in the range of 6 to 8 bits which allows 64 to 256 gray levels which corresponds to dynamic range of 36 to 48 db. This improved dynamic range produces a better B-scan image quality and data acquisition so that subtle gradation in tissues acoustic impedance can be observed and that the small portion of A-mode line could present a higher number of data points for better analysis.

During scan conversion, electronic or software interpolation of the 120 data lines provides additional data points to produce a smooth 256 line B-mode display without scan line striations and matching the given display format. Two to four data lines (256 pixels/line) are stored at one time, and the information is collected and processed to be generated in the standard raster-scan format.

Note that the user controls, as the brightness and the contrast are associated to this converter circuit as shown in figure 3.1.

The multiple independent variables involving transducer selection, instrument adjustment and scanning technique must be appropriately integrated for the creation of a technically and anatomically satisfactory scan.

The used display systems are still limited in grayscale (dynamic range) and geometrical resolutions and evolutive processing capability. This limited factors have been overcome by using a PC whose graphical display technology has been developed to a high degree to present higher quality of the image from which A-mode lines are extracted, with higher resolution and dynamic range, and then analyzed.

2-PC-based ultrasonic image processing:

Nowadays, PC-based image processing systems cover a broad range of hardware features. Basically one card is plugged into a PC which is dedicated to capture, display and processes images.

The BNC video output plug of the echograph is connected directly, or indirectly via VCR, to the input of the acquisition video card (Pixel view) incorporated in an IBM PC AT equipped .
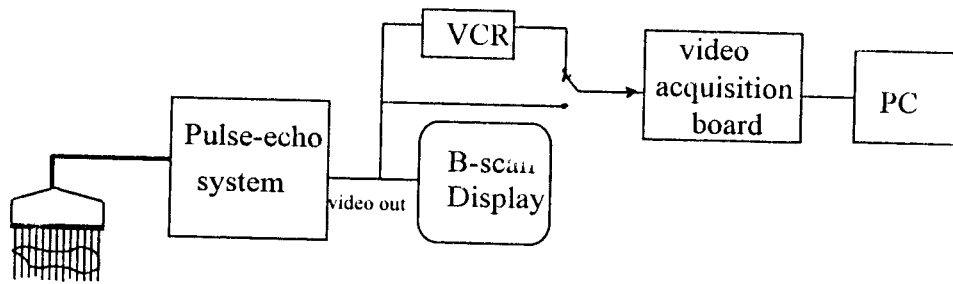
Fig-3.5 PC-based pulse-echo system

with SVGA card and a high resolution screen providing a processing and analysis station as shown in the figure 3.5. The recorded B-scan still images are captured and optimally processed in order to outline the areas of interest (AOI's).

ACOUSTIC IMAGE PROCESSING

Image processing tasks, suited to acoustic imaging are performed to highlight a particular abnormality to diagnostician to point out the suspected pathological region AOI from which data, two-dimensional-samples and a column vectors, are extracted and analyzed for pathology detection. Also, this processing may be used preliminary to identify gross diseases in the liver when visual inspection fails .

1- Introduction to clinical pattern recognition of the B-scan images

1.1- Introduction to clinical interpretation

In the interpretation of the pattern produced in the echograph screen, a detailed understanding of gross anatomy and pathology is a prerequisite. Mental extrapolation and deductive reasoning are always used and necessary. However, the most used clinical features are, consistency aspect, wall texture, back to front wall ratio , shape factor and so on...

The clinical interpretation are currently based on the visual observation of the reflection amplitude level in which doctors use the following terms for :

-The consistency analysis such as Hyper-echogene, echogenic, echodense, echomedium hypoechogene, isoechogene, Anechoic (liquidian) transonic and sonolucent;

-The wall analysis such as smooth, rough, not well defined margin .

However, close examination of clinical US scan shows it to be composed of a set of pixels. Those pixels of high amplitude often arise from organ boundaries, bones surfaces etc... The echoes arising from within the organ are relatively of lower intensity. For instance, the liver parenchyme appears as uniform medium level gray pattern, typically about 6 spots per square centimeter, with well defined edges [8].

2- Mode reflection display

The image, obtained on the screen, refers to two-dimensional reflection intensity function, denoted by f(x,y) where the amplitude at a spatial coordinate (x,y) gives the intensity (brightness) of the NxN image matrix at that point [13].

$$f(x,y) = \begin{bmatrix} f(0,0) & f(0,1) & ... & f(0,N-1) \\ f(1,0) & f(1,1) & ... & f(1,N-1) \\ & & & \\ f(N-1,0) & f(N-1,1) & ... & f(N-1,N-1) \end{bmatrix} \qquad (4.1)$$

Since the image, visualized in echography, is obtained from ultrasound reflections at tissue interfaces ; the basic nature of f(x,y) may be considered as being characterized by the following two components:

-Illumination i(x,y) which is the amount of ultrasound incident on the region to be viewed.

-Reflectance coefficient r(x,y) defined as the ratio of the reflected intensity to the incident one. The functions of $i(x,y)$ and $r(x,y)$ combine as product to form:

$$f(x,y) = i(x,y).r(x,y) \qquad (4.2)$$

where $0 < i(x,y) < i_{max}$ and $0 < r(x,y) < 1$

In the case of monochrome acoustic image, the intensity corresponds to the gray level which varies continuously from black to white. Now, the useful range of this gray scale lies from 64 to 256 levels.
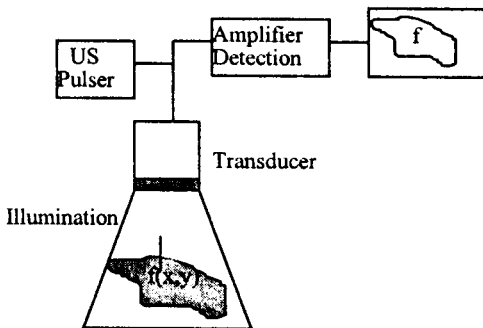
Fig-4.2 Image illumination-reflectance
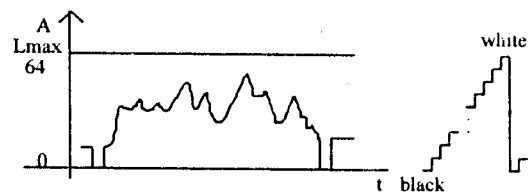
Fig-4.3 One-dimensionnal A mode line signal

With the original source of intensity supposed constant, the limit L_{max} is obtained by maximizing the reflection factor r using a perfect reflector (a mirror or a well polished metallic plate) at specular position. This could be taken be as an above reference for further determination of relative reflection. For better accuracy, each time this reference must be measuredand calibrated since B-mode examination is not repeatable.

1.2- Different clinical Aspect of masses

In fact, three fundamental clinical aspects are observed in ultrasonic cross-section of liver organ [6]: echo-free area, homogeneous echo-filled region, complex or inhomogeneous region.

1.2.1- Echo-free area

This figure can have a regular or a non-regular form with slightly parallel borders. No echo appears despite an increase in gain setting of the apparatus. This corresponds to structures such as liquid cavity, vessels and organs rich in blood which allow the beam to pass freely. Also, it should be noted that the presence of structural protein in the walls of arterial blood vessels makes them strong reflectors and that not all the fluids have a low attenuation because this depends on the concentration of the large molecules like protein of DNA.

The contours are clearly shown in some pathology cases such as hematoma, organ capsule, abscesses or Cyst. This later, that is very current, can be located because of the fluid pocket and/or homogeneous material contained within the cyst and its smooth wall texture.This produces a rounded echo-free area displayed as constant black color over its cross sectionnal area on B-scan image. In addition, bright band appears beyond it and this is due to low attenuation as shown in figure 4.1-a.

1.2.2- Homogeneous or filled area

This is displayed, using either a small or a relatively high gain, with various regular echoes showing tissular or solid structure in the liver. A cross section image may be obtained and differentiated from the rest of the organ presenting several structures by setting the TGC gain and contrast at an appropriate level as in the case of a filled neoformation , benign or malignant, which is developed in the liver. For instance, solid mass can be often located because of the potentiel homogeneous nature of the material within the tumor where an echo-filled region is produced. However, blood vessels, cancerous tissue or other inhomogeneous entities could produce many echoes from the area. Quite often an acoustic shadow is produced on B-scan behind the solid material because of the small amounts of the sonic energy that propagates beyond the solid material as shown in figure 4.1-c.

1.2.3- Inhomogeneous or mixed region

This region associates echo-free zones containing bunch of echoes, more or less limited, with a relatively echogenic and dense areas. All these zones, including sane part of liver and region showing the pathology like tumor and necrosis or abscess, are in relatively homogeneous area .
Since the differential diagnostic is done with some uncertainty, then the use of gray scale technology has lead to an improved dynamic range and a numerical evaluation of the different features providing much better accuracy of discrimination. Refer to fig 4.1-d
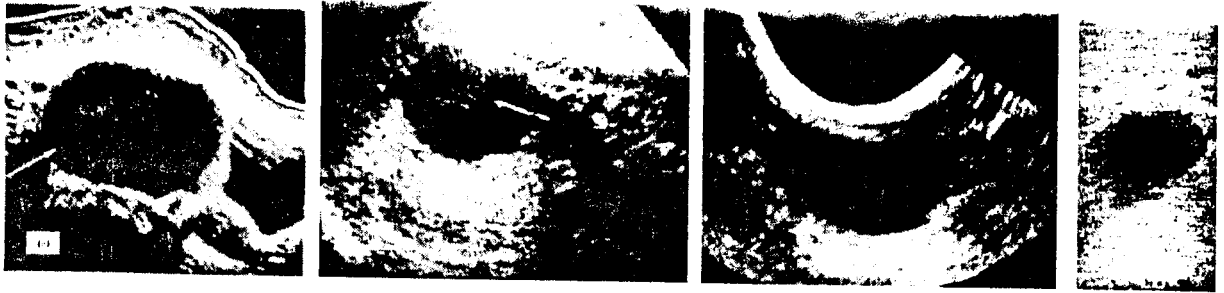
Fig-4.1-a Liquid masses or Cysts : Anechoic masses which through-transmits ultrasound freely with indication of a distal bright up.

Solid tissue mass   gallstones

Fig-4.1-b Solid masses characterized by strong reflection with acoustical shadowing.

-Right lobe of cirrhotic liver showing marqued attenuation of echo amplitude posteriorly,

Cirrhosis: the anterior portion returns high level of echoes with an altered texture. The posterior portion is poorly imaged owing to increased attenuation.

Extensive region of irregularly increased in the the right lobe of the liver. It has poorly defined margins. Metastasis from carcinoma of colon

Fig-4.1-c Malignant cancers

Multiple masses (M) which represent metastases

highly echogenic mass (M) representing metastases

Mixed mass

A typical poorly reflecting deposit with rather ill defined margins in the righ lobe of the liver.Three innocent cysts with smooth wall and increased through transmission

Fig-4.1-d Various pathologies

Fig-4.1 Acoustic images showing different pathologies, Liquid, Solid and complex masses [3,1,8].

The selection of the image matrix dimension as well as the number of the discrete gray levels are important in determining the image resolution and capacity storage. A typical size comparable in quality to monochrome pulse echo image is 512x512 array with great than or equal to 64 gray levels.

However, the use of the bitmap format is justified by the fact that windows have structures ready for use which are used directly by the bit map functions. In the file, the information about the image, color and pixels are stored in the form of data that can be read block after block to memory directly in the corresponding structures.

Each bitmap file contains a bitmap-file-header, a bitmap-information header, a color table 1 and an array of bytes that defines the bitmap pixels. The knowledge of this format will allow the conversion of the image into a gray level value matrix for further processing and A-mode column vector extraction .

3-Acoustical image processing

Some optimal image processing steps, as shown in figure 4.4, are performed for gross diseases diagnosis and meanly to outline the area of interest from which data are extracted and then analyzed for pathology identification in the examined liver organ.

The microcomputer is equipped with software program that can handle image processing tasks adapted to acoustic imaging such as edge detection, contrast enhancement,TGC , inversion,
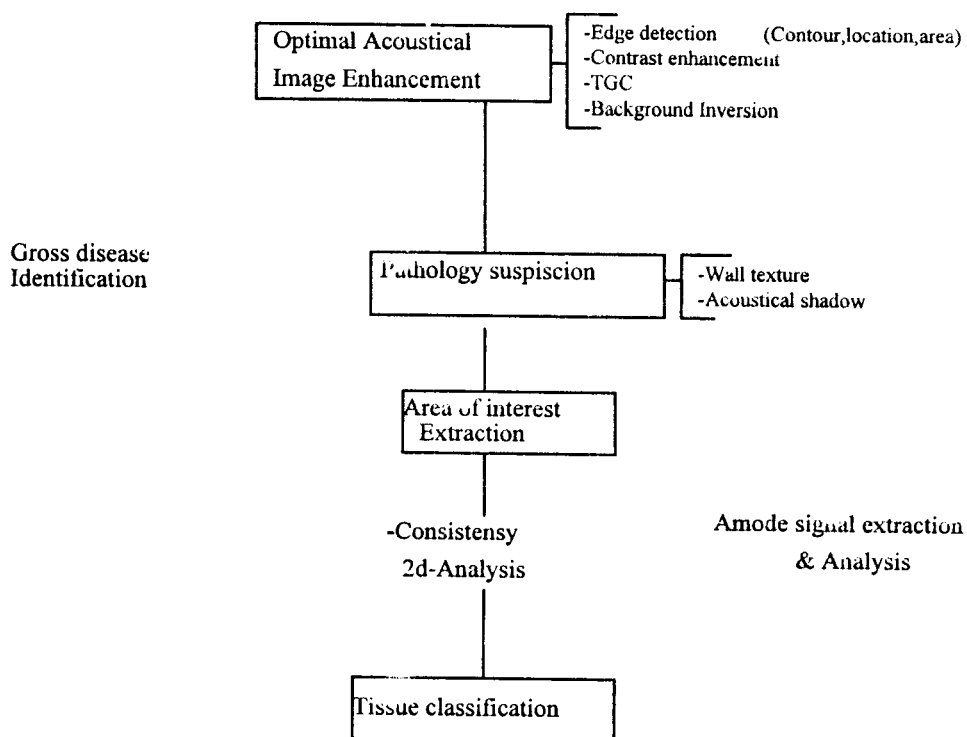

Fig-4.4   Image processing steps for pathology detection

2- Mode reflection display

The image, obtained on the screen, refers to two-dimensional reflection intensity function, denoted by f(x,y) where the amplitude at a spatial coordinate (x,y) gives the intensity (brightness) of the NxN image matrix at that point [13].

$$f(x,y) = \begin{bmatrix} f(0,0) & f(0,1) & ... & f(0,N-1) \\ f(1,0) & f(1,1) & ... & f(1,N-1) \\ & & & \\ f(N-1,0) & f(N-1,1) & ... & f(N-1,N-1) \end{bmatrix} \qquad (4.1)$$

Since the image, visualized in echography, is obtained from ultrasound reflections at tissue interfaces ; the basic nature of f(x,y) may be considered as being characterized by the following two components:

-Illumination i(x,y) which is the amount of ultrasound incident on the region to be viewed.

-Reflectance coefficient r(x,y) defined as the ratio of the reflected intensity to the incident one. The functions of $i(x,y)$ and $r(x,y)$ combine as product to form:

$$f(x,y) = i(x,y).r(x,y) \qquad (4.2)$$

where $0 < i(x,y) < i_{max}$ and $0 < r(x,y) < L$

In the case of monochrome acoustic image, the intensity corresponds to the gray level which varies continuously from black to white. Now, the useful range of this gray scale lies from 64 to 256 levels.

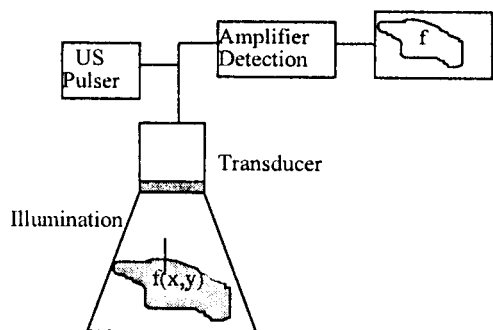Fig-4.2 Image illumination-reflectance   Fig-4.3 One-dimensionnal A-mode line signal

With the original source of intensity supposed constant, the limit L_{max} is obtained by maximizing the reflection factor r using a perfect reflector (a mirror or a well polished metallic plate) at specular position. This could be taken be as an above reference for further determination of relative

The selection of the image matrix dimension as well as the number of the discrete gray levels are important in determining the image resolution and capacity storage. A typical size comparable in quality to monochrome pulse echo image is 512x512 array with great than or equal to 64 gray levels.

However, the use of the bitmap format is justified by the fact that windows have structures ready for use which are used directly by the bit map functions. In the file, the information about the image, color and pixels are stored in the form of data that can be read block after block to memory directly in the corresponding structures.

Each bitmap file contains a bitmap-file-header, a bitmap-information header, a color table 1 and an array of bytes that defines the bitmap pixels. The knowledge of this format will allow the conversion of the image into a gray level value matrix for further processing and A-mode column vector extraction .

3-Acoustical image processing

Some optimal image processing steps, as shown in figure 4.4, are performed for gross deceases diagnosis and meanly to outline the area of interest from which data are extracted and then analyzed for pathology identification in the examined liver organ.

The microcomputer is equipped with software program that can handle image processing tasks adapted to acoustic imaging such as edge detection, contrast enhancement,TGC , inversion,

Optimal Acoustical Image Enhancement
- -Edge detection   (Contour,location,area)
- -Contrast enhancement
- -TGC
- -Background Inversion

Gross disease Identification

Pathology suspiscion
- -Wall texture
- -Acoustical shadow

Area of interest Extraction

-Consistensy 2d-Analysis

Amode signal extraction & Analysis
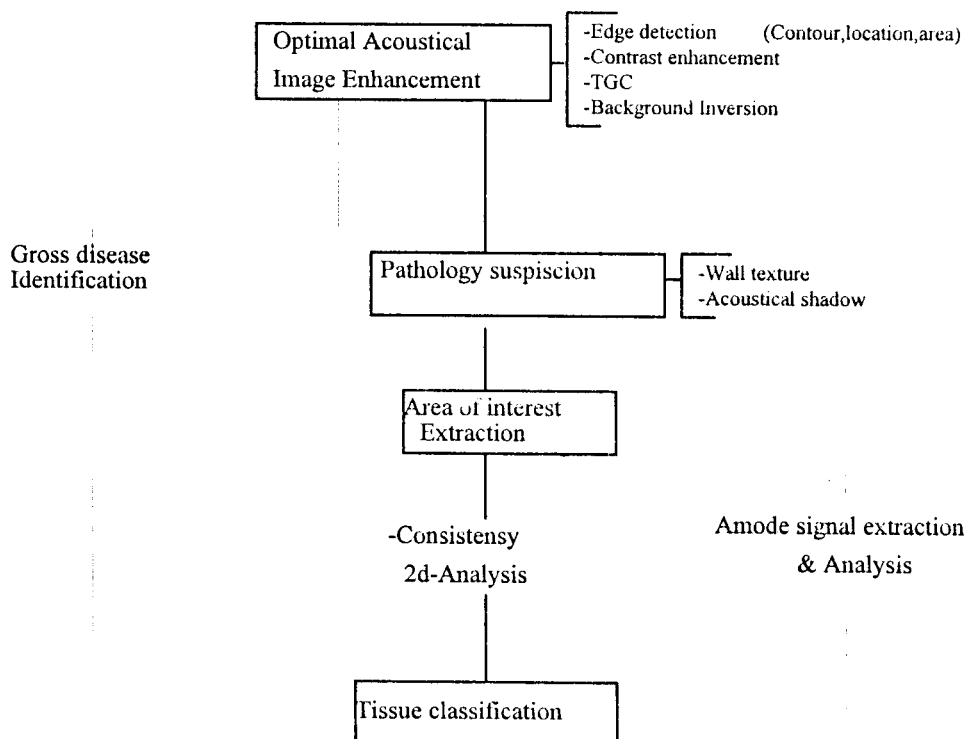
Tissue classification

Fig-4.3   Image processing steps for pathology detection

smoothing and other image processing techniques to highlight a particular abnormality to diagnostician and then to outline the suspected pathological region when visual inspection fails or is in doubt.

This processing is based in the convolution operation which enhance a particular feature of an image at the expense of others less important in acoustical image.

In the time domain this is expressed in the form :

$$g(x,y) = f(x,y) * h(x,y)$$ (4.3)

where f(x,y), g(x,y) are respectively the original and the processed image and h(x,y) the processing operation or transfer function.

For all image processing tasks that will come refer to figure 4.6 at the end of this section.

3.1- Contour detection:

Contour information is important in pattern recognition of organs such as shape, dimension and so on.., and their interrelationship as means of establishing orientation in anatomical cross section providing specular condition for the probe.

This processing aims to highlighting edges by emphasizing the changes in gray values and suppressing areas of constant gray values. This filter operation is obtained by a differentiation operation or gradient method which assumes relatively large values for prominent edges in an image, and small values in regions that are fairly smooth, being zero in the regions that have a constant gray level. The filtered image is expressed as follows,

$$G\left[f(x,y)\right] = \begin{bmatrix} \dfrac{\partial f}{\partial x} \\ \dfrac{\partial f}{\partial y} \end{bmatrix}$$ (4.3)

Once the edges are picked out, the computer can more easily determine the location and the shape of the pathological mass. This information is also useful when abnormal masses and deformations are visualized by ultrasound.

3.2- Contrast enhancement

The maximum visual contrast, which results in an enhancement of dynamic range, is technically adequate for further test of A-mode amplitude which would make a possible automatic pathology detection. This is a point operation based on histogram transformation. A contrasted image C is obtained from the acquired image I_a by a linear or logarithmic transformation function T such that each image pixel is transformed independently of all the others as,

$$C(x,y)=T(I_a(x,y))$$ (4.4)

If T is a linear function:

$$Dc=T(D_a)=a*D_a+b$$ (4.5)

where D_a is the gray level of any pixel in I_a image and D_c is the gray level of the corresponding pixel in C image [17].

The effect of different values of **a** and **b** can be described as follows:

-The coefficient **a** will control the contrast or the gain of the acoustic video signal.

If $a > 1$ then the contrast of the transformed image is increased (and is reduced if $a < 1$).

-The parameter **b** will shift the image up or down in the brightness.

This later case is corresponding to the reflection mean value and needs to be normalized.

3.3-TGC effect on the image

This user gain control setting allows one to select an appropriate correction for the average attenuation rate offered by the tissue. Where the region traversed departs from this average, an error will arise in the correction, proportional to the degree of departure and the pathlength. Where the tissue attenuation is higher, than the corrected for, a band of apparently lower echoes appears on the final image beyond the concerned area. While shadowing occurs when sufficient ultrasonic energy cannot propagate beyond the tissue-reflector being in study because of its high acoustic impedance and attenuation. The column vectors of the image are compensated as follows:

$$F_c = TGC(f(x,y))$$ (4.7)

This control is generally set in the echograph itself but it can be added in computer as an image processing task to enhance the already set compensation.

3.4- Background inversion

Some subtle structures are better visualized with either a black or white background. For example, lesions and textured organs (as liver, spleen, kidney..) in which there was a background of low level echoginity appeared better visualized using a black background. While in structures with well defined borders, such as the liver surrounding pancreas and biliary tree, the use of white background is desirable.

Also a sufficient natural positive background enables a morphological visualization of a malignant lesion as area of augmented signal strength standing out from a normal background. While in the

benign lesions a reverse negative would possibly reveal benign lesions as deficiencies in the normal background [15].

This operation consists of replacing each gray level g by its complement k in the gray scale range. For a 6-bits-coded image the inverse of initial gray level g will result in a value of k given by:

$$K = (2^6 - 1) - g = 63 - g \qquad (4.8)$$

The image inversion is obtained when this operation is applied for all pixels of the matrix.

3.5- Ultrasonic noise and artifacts and filtering

3.5.1 -Ultrasonic noise and artifacts and their recognition

The spurious noise may be caused either by the diffuse-appearing artifactual echoes or electronic noise. In the first case, the echoes are often noted within fluid-filled structures because of their intrinsically hypoechoic nature ; while in the latter one, it may occur because of the faulty equipment or transducers or because the overall system output gain is set too high. The B-scan appears to contain echoes everywhere even in known sonolucent structures. The ability to adjust finely the various controls will reduce noise artifacts and particularly by using echo level suppressor.

Regardless of the cause, any unrecognized artifact may result in scan misinterpretation and diagnostic error. Artifacts occur in many forms, including spurious echoes or shadows and pseudomasses. Pseudomass formation frequently relates to reverberative phenomena , such as multipath reflections and mirror images. Combined absorption and reflection of sound from fibrofatty tissue can also create pseudomasses, particularly in liver and spleen.

The reverberation, that is produced by multipath reflections, occurs when sound, reflected from highly curved surface, does not return directly to the transducer but undergoes additional reflections from nearby curved specular surfaces.
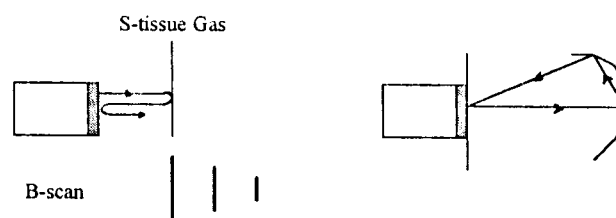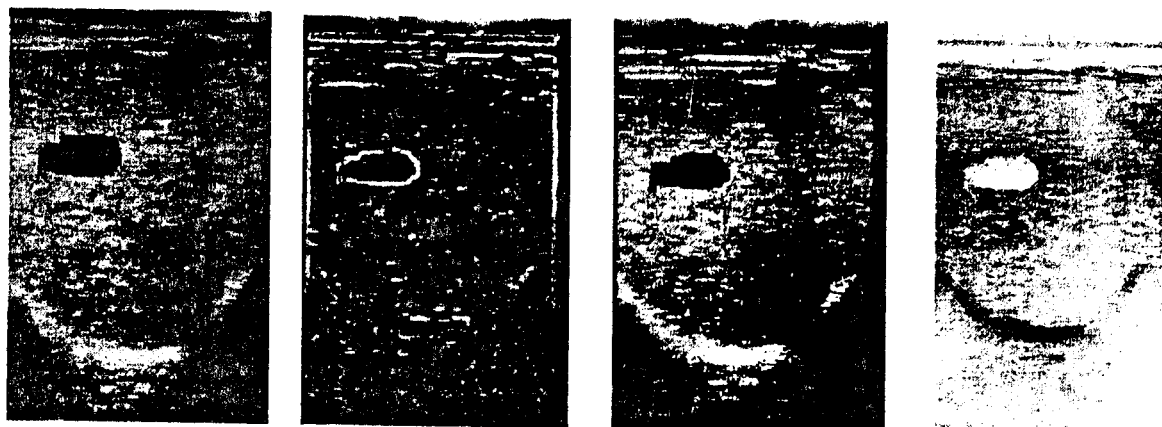

Fig-4.5 Reverberation artifacts

Acquired image   Contour detection   Contrast Enhanc.   Inversion

Smoothing   AOI delimitation   extraction
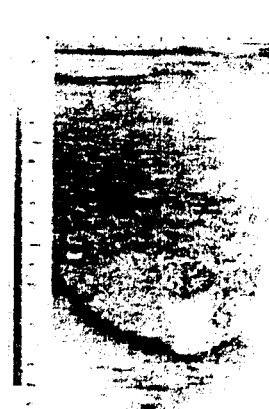
a-Case of study 1
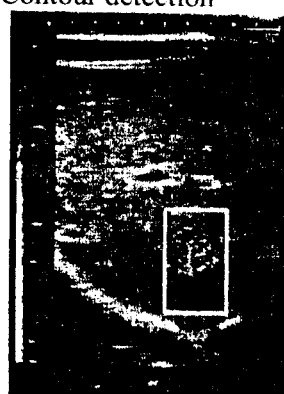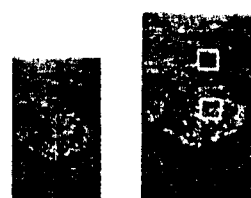
Acquired image   Contour detection   Contrast Enhanc.   Inversion

Smoothing   AOI limitation   extraction   AOI samples selection

b-Case of study 2

Fig-4.6 Acoustical image processing steps for 2 cases of study

3.5.2-Smoothing operation

This is additionally used to diminish this spurious effects that may be present in a digital image and to filter structures with high wave numbers.

This processing is obtained by an integration or averaging operation. Every point (x,y) of the generated smoothed image is obtained by averaging the gray level values of the pixels of f(x,y) contained in a predefined neighborhood of a point (x,y). The smoothed image is obtained using the following relation,

$$g(x,y) = \frac{1}{M} \sum_{(n,m) \in s} f(n,m)$$

(4.9)

For $x,y = 0,1,2.......N-1$, S is the set of coordinates of points in neighborhood of point (x,y), M is the total number of points in the neighborhood.

Other processings like zooming and color processing could be considered . The magnification of portion of the image, that is obtained by pixels duplication, permits to recognize visually the internal consistency texture of the organ and differentiate tissues from pattern recognition of their spatial distribution of the echoes in organs; while the color processing offers some significant benefits to medical vision system by coloring gray scale image to enhance a particular details using gray to color map operation or some look up table.

4-AREA OF INTEREST (AOI)

The several previous image processing can probably lead to the localization and delimitation of area(s) of interest such as the suspected rectangular one for processing .
This cropped AOI should include three subregions which are:
- A normal region of the liver that will be the local reference for comparison.
- A region of the lesion .
-A region beyond the lesion for further attenuation estimation.

4.1-One-dimensional column vector extraction

Once the AOI is converted to a gray level matrix, individual column vectors, repr... ...ng the A-mode lines, are selected , extracted to be further analyzed on the base of their amplitude weights for pathology recognition .

$$As = \begin{bmatrix} f(0,s) \\ f(1,s) \\ . \\ . \\ f(N-1,s) \end{bmatrix}$$

<div align="right">(4.10)</div>

where A_s is the selected A-mode line at s^{th} column vector.

4.2-Two-dimensional sample extraction and analysis

Alternatively, sample areas are extracted , as a biopsy, from normal and pathological regions and analyzed using textural techniques based on statistical (averages) and spectral (homogeneity) approaches. The consistency is best analyzed in two dimension-mode because the number of data points of the considered area is higher and this leads to the diagnostic result of high probability.

4.2.1- Histogram

This is a statistical operation that produces a count of the number of pixels of each intensity in image enabling further averages calculation and providing an echo amplitude distribution.
The histogram $H(D_i)$ is a graph of number of pixels with gray level D_i, where $0 < D_i < 64$;
By summing over a number of pixels ,the histogram becomes integral:

$$S = \sum_{i=0}^{63} H(Di)$$

<div align="right">(4.11)</div>

4.2.2- Reflection mean

Shawker and Al were able to diagnose focal or diffuse liver diseases when visual inspection failed [2] sing a simple histogram algorithm of calculation of the echo amplitude average in a specified region,

$$M_R = \frac{1}{M.N} \sum_{x=1}^{M} \sum_{y=1}^{N} f(x,y)$$

<div align="right">(4.12)</div>

4.2.3- Spatial distribution density

This is an evaluation of the number of reflections of given peak value per unit surface. In another word, this is a number of pixels with gray level value greater or equal than a given level D_L over the total number of pixels of the rectangular sample area expressed as ,

$$S_{dd} = \frac{\sum\limits_{\substack{i=1 \\ D_i > D_L}}^{M.N} H(D_i)}{M.N \ \text{(pix)}} \qquad (4.13)$$

Note that a surface of 1cm² corresponds to 20x20 pixels

4.2.4- Variance

The variance of the trace is of particular importance in texture description[13]. It is a measure of gray level contrast that can be used to establish descriptors of relative smoothness given by the following coefficient,

$$R_c = 1 - \frac{1}{1 + \sigma^2} \qquad (4.14)$$

For example , the measure of R_c tends to 0 for an image of constant intensity or smooth texture and approaches 1 in the case high coarseness.

4.2.5- Results and comments

4.2.5.1- Results
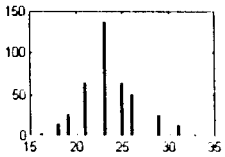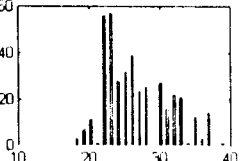
Tissue sample	Mean M (gray level)	Spatial distr. Sd	Smoothness Rc	Histogram
Normal liver	24	14	.90	
Pathological mass	27	91	.95	

Table 4.1 Results of 2D-sample analysis of one pathological case.

4.2.5.2-Comments

Relative to a normal liver sample, this pathological mass sample indicates in Table 4.1 a higher reflection mean with an histogram weighted to the right. Also, it has much greater spatial distribution density and it is of less smoothness. Therefore, this sample could be considered as being of solid tendency.

A-MODE SIGNAL PROCESSING ANALYSIS

1-The model of A-mode signal

When excited by a high voltage pulse, the ultrasonic transducer produces a wavelet that will be transmitted into the human tissue that is composed of a series of n interfaces acting as reflectors [3] as shown in Fig-5.1.

Tissue interfaces
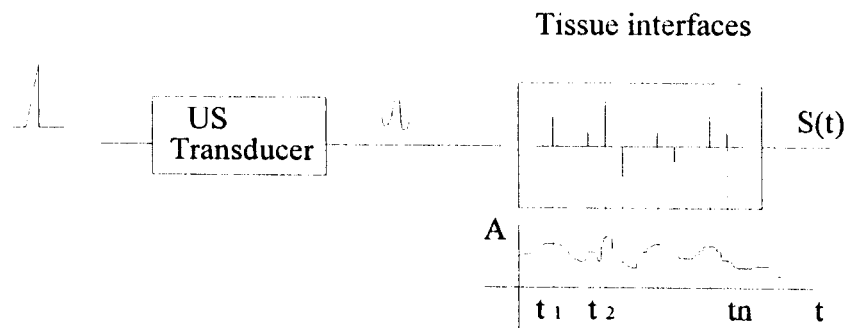
Fig-5.1 System modeling for A-mode signal tissue reflection

The transducer will receive, from these reflectors, a series of impulse responses at times t_i having the form,

$$R_1 w(t - t_1), R_2 w(t - t_2) ... R_i w(t - t_i)$$

where R_i and $w(t-t_i)$ are respectively, the reflection coefficient and the weight of the wavelet at the ith reflector.

The overall response produces a trace $S(t)$ that is expressed as,

$$S(t) = \sum_{i=1}^{n} R_i . w(t - t_i) \tag{5.1}$$

$S(t)$ is considered as the output of an n-order linear system excited by wavelet $w(t)$, whose impulse response is the series of reflection coefficient R_j.

The present pulse-echo systems are based on the envelope detection method and therefore a low pass filter is used to suppress the carrier and the RF noise to end up with the envelope that is a monodimensional A-mode trace given as,

$$A(t) = S(t).H_{pe}$$

(5.2)

The reflected ultrasound beam is detected in the form of energy and since it is gated, the obtained A-mode signal is considered as a finite energy signal

2- Preliminary A-mode signal processing

The consideration of different regions of the same liver organ, with the normal one taken as the local reference, as well as the use of the same ultrasonic beam path should allow an efficient tissue differentiation.

The processing operations such as normalization, gating the trace of interest (TOI) and the correlation are performed preliminary.

2.1- Normalization and TGC compensation :

The user controls such as the brightness and the contrast affect widely the signal parameters such that the obtained signal will not reflect the original one (refer to Chapt.3).

This normalization operation will bring mainly the values of the reflection mean of the displayed trace portion A_r.corresponding to that extracted from the normal region in liver to the calculated liver reference value 12.5 dB obtained from the graphical distribution in Fig2. 4 The the overall trace As is shift up or down depending on their difference. The normalized trace A_n is then evaluated as ,

$$A_n = A_s(t) - (mean(A_r) - 12.5)$$

(5.3)

On the other hand, for the attenuation compensation, the choice of a non linear function , exp(x) or log(x), or a linear one with variable slope depends on the case of study. The compensated trace is expressed as,

$$A_c = A_s(t).TGC$$

(5.4)

This will just complement the user compensation set up at the pulse echo system.

2.2-Time gating

Time gating is used to take portions of interest (TOI) out of the selected trace A_s in the AOI for a both consistency and boundary analysis. The gated signal is expressed as follows,

$$Ag\ (t,to) = A_s(t)\ .t_w\ (t-to) \tag{5.5}$$

where t_w is the time window.

The trace $A_s(t)$ is time gated into normal, abnormal and beyond abnormal regions for consistency analysis and correlation. For the consistency fine selection, the time gate within the range of 13 to 26 µs , corresponding to a time of flight of distance 1 to 2 cm, is suitable for echo video signal analysis for early detection of cancer [7].

On the other hand, walls traces of interest (TOI), that constitute interfaces between these consistencies, are also gated for further boundary and attenuation analysis.

2.3-Correlation

A frequently used method of comparing two finite energy signals is by computing their correlation function which is defined as [11],

$$R_{A_nA_p}(m) = \sum_{n=0}^{N-m-1} A_r(n)A_p(n+m) \tag{5.6}$$

where $A_r(n)$ is a signal at time n and $A_p(n+m)$ is another (or pathological) signal at time $(n+m)$.

The correlation function is performed to measure the degree of similarity between the measured trace in the suspected area and the trace in the sane liver region considered as local reference.It is common to express correlation in terms of the following ratio given as,

$$\rho_{xy} = \frac{\sigma_{xy}}{\sigma_x \sigma_1} \tag{5.7}$$

where $-1 \leq \rho_{xy} \leq 1$ and ρ_{xy} is called the correlation coefficient and $x=An$ and $y=Ap$.

Sample estimates of ρ_{xy} close to unity in magnitude imply good correlation ,while values near zero indicate a little or no correlation.

3-A-extraction and analysis of A-mode signal Features

The A-mode signal pattern recognition skills play an important role in arriving at reliable diagnosis of inclusions or focal diseases using most of the time both the boundary and the consistency features.These two last parameters, which are indicative of the pathology, are expressed in terms of the signal parameters [5] such as amplitude averages, peak values, frequency content and so on, as summarized in the Fig-5.2 ,below,
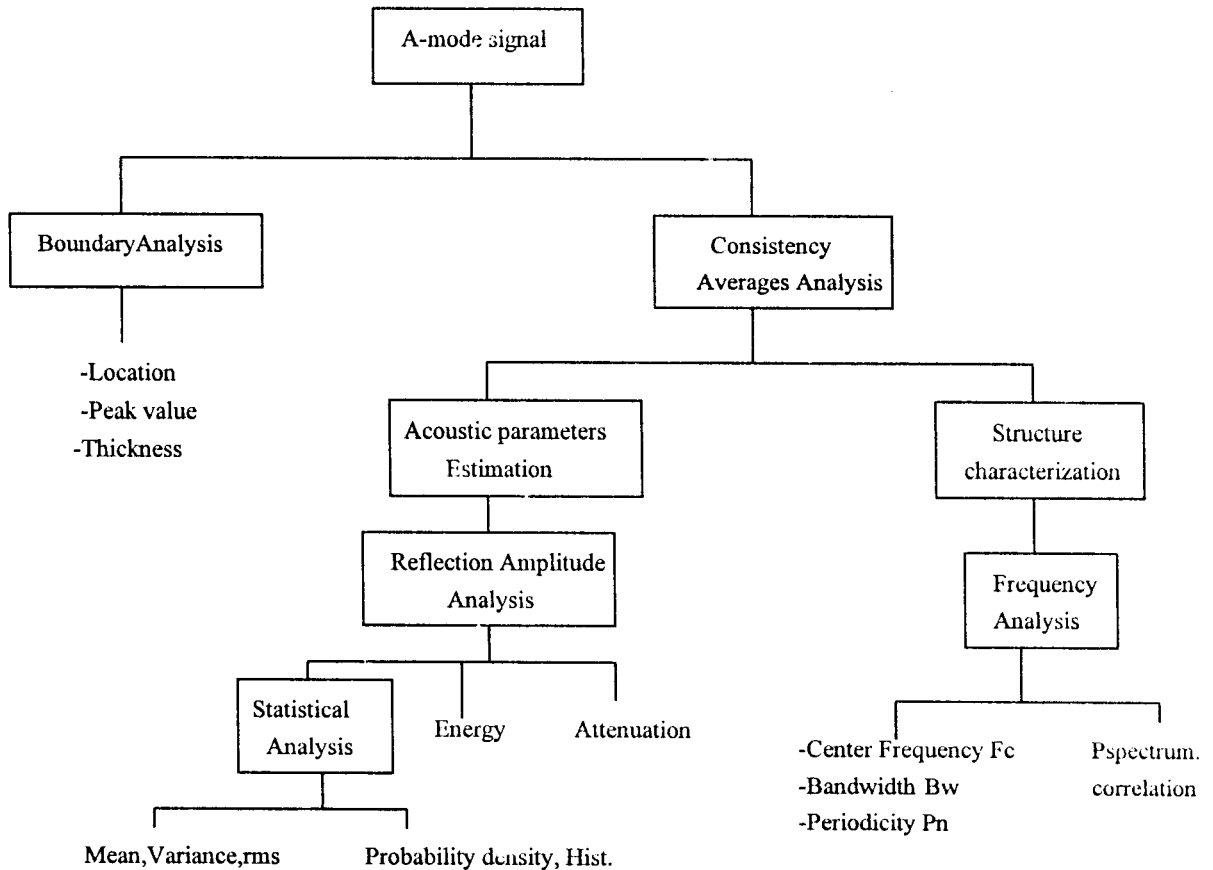
Fig-5.2 A-mode signal features analysis tree

These features are first used for tissue classification, liquid-solid-mixed, and then for characterizing the pathology, malignant or benign .

3.1- Boundary Analysis

The peak value, the thickness and the nature of the back and front walls may identify the type of pathology. This applies most of the time to focal diseases such as cyst which has a smooth wall or a solid disease as hematoma which has a rough one[6].

The boundary peaks value are best analyzed in the case of one dimensional A-mode signal.

3.1.1-Wall location

The wall of the pathology may be located as a positive or negative reflected level transition(s) which depends on its acoustic impedance relative to the normal liver medium.
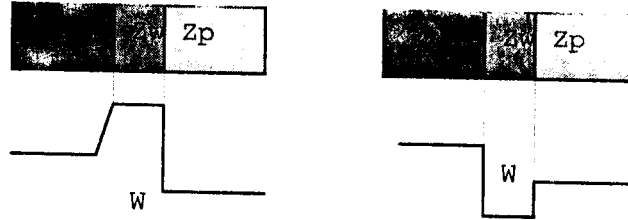
Fig-5.3 Walls detection

This detection is obtained by a differentiation operation or gradient method which assumes relatively large values for rapid transition in the A-mode signal.

Besides, once the walls are detected the pathology size could be derived. It is known, from physics, that each of a liquid , a mixed or a solid mass has a marked variation in size which depends on its evolution with time [1]. This variation is evaluated as the distance separating the back to front walls, in our case X_p. Also, it may be used for the evaluation of the overall attenuation for the lesion as well as its spatial distribution.

3.1.2- Peak value analysis

An A-mode signal, that is taken off from a region with numerous changes in brightness or in gray-level, would appear as a series of active peaks of different values. The evaluation of the relative higher peak values reflected at a particular point or laps of time $[t_1 \ t_2]$, is efficiently used for an initial profile comparison and further tissue classification. Hence the peak values of the gated signal portion, corresponding to the front or back wall , is evaluated as follows :

$$A_{wp}=max \ A(t) \qquad , \qquad t_1<t<t_2 \qquad (5.8)$$

The echo strength of a distal wall may be used to characterize the wall nature on the base of the acoustic impedance relative to that of the normal liver. While the strength ratio of the back to front walls peak values, A_b and A_f, can identify the type of the pathology by an estimation of the attenuation relative to the normal liver data, that is given as,

$$R_w= A_b / A_f \qquad (5.9)$$

If $R_w >$ 1, it corresponds to a higher reflection amplitude in the trace beyond the lesion, and therefore, the lesion presents a lower attenuation than the sane liver.

If $R_w <<$ 1 , this corresponds to a lower reflection amplitude producing an acoustic shadow, and hence ,the lesion presents a higher attenuation than the normal liver.

If $R_w \cong$ .5 <1, this corresponds to a quite low reflection amplitude producing an middle acoustic shadow, and hence ,the lesion presents medium attenuation with respect to the normal liver.

3.1.3-Wall nature analysis

3.1.3.1-The wall thickness:

This parameter is important in differentiating between pathologies and is expressed as the product of time duration and the ultrasonic speed c as:

$$T_w = (T_h - T_l).c \qquad (5.10)$$

where T_l and T_h are respectively 6db lower and higher time wall limits found by solving ,

$$A(t) = 1/2 \max(A_w) \qquad (5.11)$$
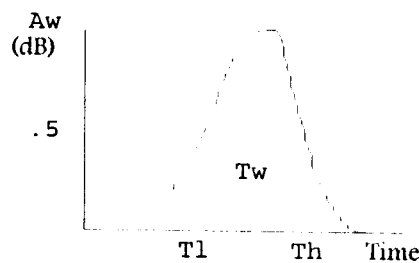
Fig-5.4 - Wall thickness

If T_w is found to less than 3mm , this case corresponds to a cystic wall.

If T_w is found to be greater than 3mm , it corresponds to a solid mass wall.

3.1.3.2-Wall nature

The rough wall is a one which contains asperities and behaves as a diffusing interface in all directions included that towards the probe. For this reason, the wall thickness is expected to be larger, with a relatively lower reflection amplitude and a higher periodicity due to diffusing in the echo beam according to eq. (2.31). On the other hand, a larger wall may be seen as wall consisting of line segments called edgels, having magnitude and direction.

These edgels correspond to discontinuities in the displayed intensity and the corresponding function, that is of nth order discontinuity, has a delta function at its nth derivative that is expressed as,

$$\frac{d^n A_w}{dt^n} = \delta \qquad (5.12)$$

As an example, a step, a linear and roof edges have respectively zero, first and second order discontinuities.

3.2-Consistency Analysis

Among the signal features of high confidence that are used to characterize the consistency, we may quote :

- The mean of the reflection amplitude obtained from the probability density function and the reflection energy .
- The estimated attenuation
- The frequency contents
- The periodicity and /or the spatial distribution .

3.2.1- Characterization using acoustic parameters estimation

3.2.1.1- Reflection amplitude analysis

3.2.1.1.1- Statistical reflection amplitude analysis

Since the internal architecture of the tissue is stochastic in terms of acoustic scattering properties then, any change in acoustic impedance is expected to occur randomly. But, in the case of the liver tissue which may be considered as homogenous medium, the obtained traces could be deterministic with some degree of ramdoness due to some abnormal phenomenon in pathological tissue.

However, an accurate statistical determination of the averages for the A-trace, enables a quantitative characterization of a particular biological tissue. This is best characterized by its probability density function and its averaging measurements.

The histogram $H(g_i)$ of a displayed column vector A is a graph which gives the number of pixels of the same value in each gray class g_i , where $0 < g_i < 64$.

It is obtained by summing over a number of pixels as,

$$N = \sum_{i=0}^{i=63} H(gi) \qquad (5.13)$$

To obtain a graph of the probability density function P(A), the histogram is first converted to a bar chart and then, a curve fitting process is carried out. The various statistical descriptive measures of the A-trace are given by the nth moments that are defined as,

$$\mu_{\kappa} = E[A^{\kappa}(t)] = \sum A^k P \qquad (5.14)$$

However , the considered process is limited to the second order, that is, the reflection mean and variance .

The first moment, which is the reflection amplitude mean, describes how the reflection process behaves on the average, and it is given by the following integral ,

$$\mu_1 = E[A(t)] = \sum A. P \qquad (5.15)$$

The mean μ_1 ,that is also the measure of the central tendency, is defined by statistics as,

$$\mu_1 = \frac{1}{n} \sum_{i-1}^{n} A_i \qquad (5.16)$$

The variance, that is the second moment, is the measure of the variability or the deviation from the mean and it is given by,

$$\mu_2 = \sigma^2 = E[(A - \mu)^2] = \sum (A - \mu_1)^2 P \qquad (5.17)$$

The sampled variance is ,

$$\sigma^2 = \frac{1}{n} \sum_{1}^{n} (A_i - \mu)^2 \qquad (5.18)$$

This measurement is related to the contrast property in the signal and tends to 0 if the points have the same value and to large values in the case of high variablity in the signal.

Other statistical values as the Rms, the skewness the reflection range can be taken into account in some cases. For instance, the RMS value , that is the square root of the variance provides a useful information about the received ultrasonic average power.
Refer to appendix C for the obtained results.

The reflection amplitude varies considerably with time and a convenient representation that reflects these amplitude variations is the short time energy. The measured total amount of the received sonic energy , that is the area sustended by the trace, is evaluated as the sum of the squares of its amplitudes A_i [15]that is ,

$$E_n = \sum_{i=0}^{l}[A_i]^2$$ (5.19)

The comparison index I_e is evaluated as to be ratio of the detected abnormal energy E_{np} to the normal or reference one E_{nr} that is given by:

$$I_{en} = \frac{E_{np}}{E_{nr}}$$ (5.20)

3.2.1.2 -Estimation of the attenuation in reflection mode

For the given values of frequency $F=3.5$ MHz and the attenuation coefficient of the liver $\alpha=.5db/cm.Mhz$; from the use of equation (2.44), the attenuation α_p , in the case of a consistency without internal interfaces, is estimated as ,

$$\alpha_p = \alpha_c - \frac{A_{R2} - A_{R1}}{FX} = 0.5 - \frac{A_b - A_f}{3.5X}$$ (5.21)

In the case of a consistency with some interfaces of the same type, and whose number may be approximately equal the periodicity value P_n , the attenuation α_p is evaluated as follows:

$$\alpha_p = 0.5 - \frac{(A_b - A_f)}{3.5.X} + \frac{P_n.Log(1 - R^2)}{3.5.X}$$ (5.22)

3.2.2-Structure characterization using reflection frequency analysis

3.2.2.1- Power spectrum analysis

The frequency profile is often used as a frequency signature for characterizing various materials and structures. The observed spectrum is a consequence of interference between Huygen's secondary wavelets originating from the interfaces or edges. It appears of significant values for tissue classification because it has the ability to make distinction between biological

structures, phenomena and sources whose frequencies are very close to each other and also it is closely related to the measurable quantities.

In pathological cases, ultrasonic video signal reflected respectively from benign or malignant may not be differentiated in the time domain while transformation in the frequency domain could provide us with possible visual discrimination . For instance, the FFT characteristic of the signal from malignant tissue could contain discontinuities .

The N points discrete Fourrier transform is given by ,

$$X(i+1) = \sum_{k=0}^{N-1} A_{k+1} \exp(2\pi j(ik / N))$$

(5.23)

For i = 0 ,....,N-1

The power spectral density $P(f)$ of a signal is a measure of the signal energy at different frequencies, and it is given by,

$$P(f) = |X|^2 = XX^*$$

(5.24)

where $|X(f)|^2$ could be considered as an energy per unit bandwidth. By integrating over the useful frequency interval from 0 to 3 MHz, we can calculate the portion of energy lying within this interval. A gating technique is often used to select a portion of the signal frequency spectrum that contains the most valid data.

Also, in the textural analysis, the fine texture will have $P(f)$ characterized by high amplitudes in the low frequency signal, while coarse texture in which gray level variations are fast and close the $P(f)$ will present high intensities in the high frequency range.

In consequence, the center frequency F_c could be evaluated as the average of the square of the FFT[9] given by,

$$F_c = Mean((FFT)^2) = \frac{\sum_{k=0}^{(N/2)-1} P_k F_k}{\sum_{k=0}^{(N/2)-1} P_k} = \frac{\sum_{k=0}^{(N/2)-1} P_k k\left(\frac{f_s}{N}\right)}{\sum_{k=0}^{(N/2)-1} P_k}$$

(5.25)

where P_k is the power spectrum and f_s is the sampling frequency.

Similarly, The RMS bandwidth B_w is evaluated as the variance of the square of FFT[9],

$$B_w^2 = \sigma^2 = \frac{\sum_{k=0}^{(N/2)-1} P_k (F_k - F_c)^2}{\sum_{k=0}^{(N/2)-1} P_k} = \frac{\sum_{k=0}^{(N/2)-1} P_k (k\left(\frac{f_s}{N}\right) - F_c)^2}{\sum_{k=0}^{(N/2)-1} P_k} \qquad (5.26)$$

Also from the spectra it is possible to extract the information on the attenuation as a function of frequency. It was shown that the evolution of the instantaneous frequency along an A-line is directly related to the attenuation of the tissue. This attenuation is increasing with frequency and the spectral content is modified with the depth. It was observed that there is a local decrease of this frequency mean with the attenuation. For example, an important drop of the center frequency, in the order of 500 KHz, for a sane liver could be observed using standard transducer of 3 MHz fundamental frequency [16].

Also, the power spectrum is used to detect global periodicity in the trace by identifying high energy, narrow picks in the spectrum. Prominent peaks in the spectrum give the principal direction of the texture pattern while the location of the peaks in the frequency axis gives the fundamental spatial period of the pattern [13].

3.2.3.3-Autocorrelation and periodicity evaluation

3.2.3.3.1-Autocorrelation

This is a measure of variability in the A-trace and it is expressed as following [11],

$$R_A(m) = \sum_{n=0}^{N-m-1} A(n) A(n+m) \qquad (5.27)$$

The more fluctuations exist in the signal, the less correlation between the neighbor points ,and hence, the more impulsive looking the autocorrelation appears. The autocorrelation function will exhibit the basic trend at the expense of the detailed information. It is capable of depicting periodicity buried up to 40 db in random signals.

On the other hand the computed normalized autocorrelation may be used to determine the degree of the regularity in the signal and then expressing that of the homogeneity in the tissue.

Note that the autocorrelation function can be obtained by the inverse transform of the power spectrum density.

This simple method is achieved by preselecting an echo amplitude level and determining the number of times the trace crosses such level. This is defined as the number of cycles present in the trace for a given time window T_{wi} .

A zero or a level crossing takes place if the measured samples have different algebraic signs. Thus, the rate at which this level crossing occurs, is the periodicity of the A-trace that can be evaluated as follows ,

$$P_n = \frac{1}{2} \sum_{n=0}^{+\infty} |sign[A(m)] - sign[A(m-1)]|$$
(5.28)

where $sign[A(m)] = 1$ for $A(m) \geq 0$

and $sign[A(m)] = -1$ for $A(m) < 0$

Consequently, the spatial distribution could be evaluated as the ratio of the number of periods to the pathology size X_p, and is given by ,

$$S_d = \frac{P_n}{X_p}$$
(5.29)

This can give information on the arrangement of the peaks in the trace for further description of the structure based on regularly spaced reflection interfaces.

4-Combination classification

A basic form of classification process consists of a data acquisition system a feature extractor and a classifier as illustrated in figure 5.5, below ,
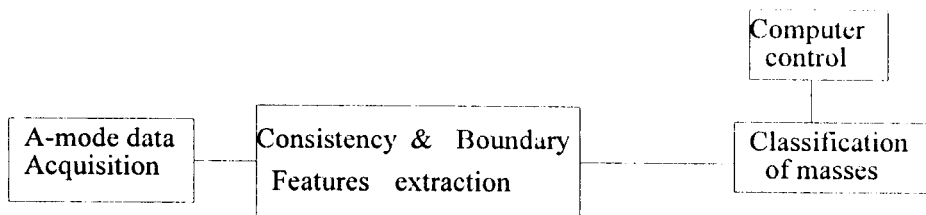

Fig-5.5 Basic form of a classification process

Let us consider the problem of determining whether a mass observed on a B-scan is either fluid- filled (cystic), solid (tumor) or mixed .

The consistency and boundary nature of medical masses are expressed in terms of the signal features whose combination is used for tissue classification (liquid-solid) and pathology characterization (malignant or benign). A logical combination tree diagram has been elaborated as shown in the figure 5.6 for a final diagnostic decision .

Let the function F_C represents a set of parameters (R, α, Sd) which are used for the consistency differentiation.

Let the reflection parameter value be presented fundamentally by three interval classes of liquid-soft tissue and solid according to the distribution given in the Figure 2.4 ,

Reflection amplitude (dB)

$$R = \begin{cases} R_L = \left\{ \mu_1 \ / \ \mu_1 < 5 \right\} & \text{liquid class} \\ R_{ST} = \left\{ \mu_1 \ / \ 5 < \mu_1 < 13 \right\} & \text{Sof tissue class} \\ R_S = \left\{ \mu_1 \ / \ \mu_1 > 13 \right\} & \text{Solid class} \end{cases} \tag{5.30}$$

Again the class R_L and R_S could be represented respectively by the following subclasses , soft tissue , semi-liquid and solid - solid tendency ,

$$R_{ST} = \begin{cases} R_{ST1} = \left\{ \mu_1 \ / \ 5 < \mu_1 < 8 \right\} & \text{Semi - liquid class} \\ R_{ST2} = \left\{ \mu_1 \ / \ 8 < \mu_1 < 13 \right\} & \text{Soft tissue class} \end{cases} \tag{5.31}$$

$$R_S = \begin{cases} R_{S1} = \left\{ \mu_1 \ / \ 13 < \mu_1 < 16 \right\} & \text{Solid tendency} \\ R_{S2} = \left\{ \mu_1 \ / \ \mu_1 > 16 \right\} & \text{Solid} \end{cases} \tag{5.32}$$

where the inferior and the superior limits are obtained from the same figure.

Similarly, the attenuation parameter is also represented by three classes according to figure 2.6 ,as follows,

$$\alpha = \begin{cases} \alpha_L & \text{for } \alpha_p \leq .2 & \text{liquid} \\ \alpha_{st} & \text{for } 0.2 \leq \alpha_p \leq 2 & \text{Soft tissue or Mixed} \\ \alpha_s & \text{for } \alpha_p > 2 & \text{Solid} \end{cases} \tag{5.33}$$

The other way of presenting approximately these attenuation classes is to use the reflection walls ratio:

$$R_w = \begin{cases} r_{wL} & \text{for } r_w \geq 1 & \text{liquid} \\ r_{wst} & \text{for } .1 < r_w < 1 & \text{soft tissue or mixed} \\ r_{ws} & \text{for } r_w \ll 1 & \text{solid} \end{cases} \qquad (5.34)$$

The Spatial distribution Sd or the Periodicity P have the following possibilities, which are,

$$S_d = \begin{cases} S_{drr} & \text{for } S_d = S_{dr} \\ S_{d1} & \text{for } S_d > S_{dr} \\ S_{d2} & \text{for } S_d < S_{dr} \end{cases} \quad \text{or} \quad P = \begin{cases} P_r & \text{for } P_n = P_r \\ P_1 & \text{for } P_n > P_r \\ P_2 & \text{for } P_n < P_r \end{cases} \qquad (5.35)$$

Where S_{dr} or P_r is the liver local reference spatial distribution or periodicity.

The sample set corresponding to the consistency function F_c is given by the following product,

$$F_c = R \times \alpha \times S_d \qquad (5.36)$$

and then the number of possible consistency outcomes is,

$$Nc = 3.3.2 = 18 \qquad (5.37)$$

The function Fc with set of conditions:
- (R_L, α_L, S_{d1}) corresponds to liquid class consistency function F_L
- (R_S, α_S, S_{d2}) corresponds to solid class consistency function F_S

On the other hand, let F_w be a function of a set of boundary parameters (T_w, P_k,..) where the Wall thickness is represented by,

$$T_w = \begin{cases} T_1 & \text{for } T_h \geq 3mm \\ T_2 & \text{for } T_h < 3mm \end{cases} \qquad (5.38)$$

and the relative peak value, by,

$$P_k = \begin{cases} P_{k1} & \text{for } P_k > P_{kr} \\ P_{k2} & \text{for } P_k < P_{kr} \end{cases} \qquad (5.39)$$

Boundary

Consistency

thickness
Th

peak value Nature
Pk

Attenuation
estimation

Size   Homogeneous

Inhomogeneous
xInterfaces

Fw

Fc

Pk1   Pk2

Back/Front A
Rw

Echo free area
Fl

Echo filled area

<3mm   >3mm
T2   T1

liquid

Fs   Fst
solid   Soft tissue

Fm
Mixed area

>=1   <<1

Enhancem. Shadow

CYST

Benign
Cancer

Malignant
Cancer

Normal
liver tissue
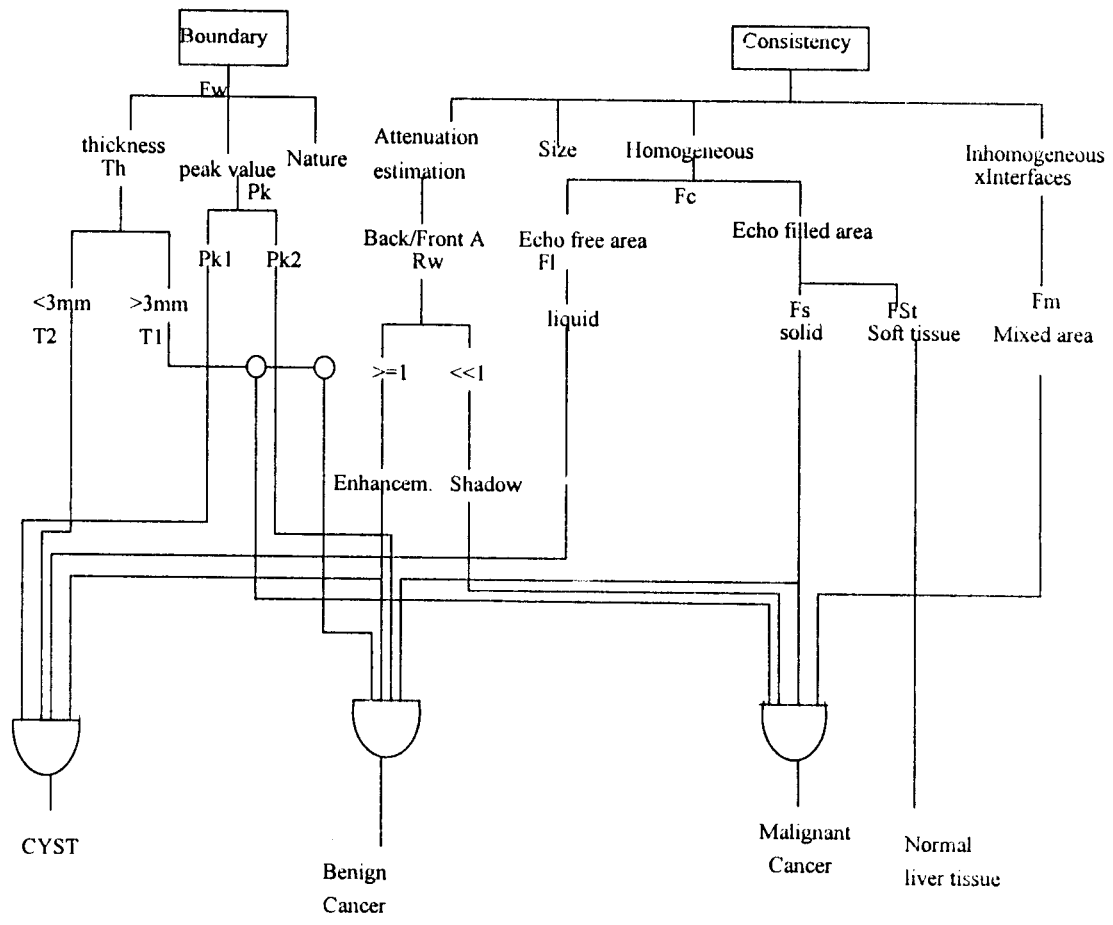
Fig-5.6 Decision tree for pathology classification

For example, the function F_w with walls states (T_2, P_{k1}) corresponds to a calcified smooth wall while F_w with (T_1, P_{k2}) corresponds to a rough wall .

The diagnosis function F_d for the focal decease's could be expressed as a combined sample of the consistency and the boundary functions denoted by:

$$F_d = F_c \times F_w \qquad (5.40)$$

Hence, the number of possible diagnosis outcomes is evaluated as,

$$N_d = 18.4 = 72 \qquad (5.41)$$

Some examples of pathologies obtained by the combination of the previous parameters are given in table 2 of Appendix C.

5-Interpretation and discussion of results

Since our first objective is to differentiate between liquid and solid masses representing respectively 60% and 30% of liver decease's [1], two corresponding AOIs , which are shown in table 5.2, have been considered. Data within tables 5.3 and 5.4 have been obtained from mathematical analysis that has been presented in previous sections. Using these data in conjunction with the curves in table 5.2, the following discussion may be presented for both case studies 1 and 2.

-Pathology Case 1

The correlation coefficient and the corresponding graphical representation in table 5.1 shows that there is no correlation between studied traces.

The small value of the reflection mean ($\mu_l=2.59$ dB) ranges within the values which correspond to a liquid class according to figures in table 5.2. However, the small variations in the curve of the trace, due to some spurious echoes, will give a meaningless periodicity. Furthermore, the value of ΔR , which is positive in this case, estimates the value for the attenuation α_p to be lower than that of the liver and it tends to be in the range of that of a liquid. The estimated values for the parameters μ_l and α_p , which are of high confidence , will classify this consistency as a *liquid*. On the other hand, the value of the *wall* thickness T_W , which is less than *3mm*, indicates the presence of a smooth boundary, whereas, the higher value for the reflected peak of the front wall shows a calcified wall [7]. therefore , it is deduced that this pathology is a cyst.

For pathological case 1, The power spectrum shows more high frequencies while the autocorrelation grahics in table 5.5 indicates faster and small fluctuation in the trace than that of the normal liver. This may be refered to remaining noisy echoes in the considered mass.

Their combination leads to the following diagnosis function written as,

$$F_d = F_L \times F_{ws}$$ (5.42)

which leads to a cystic mass diagnosis.

-Pathology case 2

The near zero value of ρ_{xy} in table 5.1 shows that the studied traces are very different; while the autocorrelation, in table 5.5, is characterized by more fluctuations, due to more interfaces, in the trace of case 2 than that of the normal liver .

The regularity of the trace in case 2 shown in table 5.2 indicates that this pathology is homogeneous. The average value of the reflected amplitude, that is, about *two dB's* greater than that of a normal tissue, indicates a relatively higher acoustic impedance. Also, the higher value of the periodicity in table 2, shows the presence of multiple echoes or interfaces. The amplitude of the back wall echo is much smaller than that of front wall indicating a higher attenuation. In addition to this, we can notice from the previous tables that the walls' thickness ranges critically at *3mm* indicating that their nature is more or less a rough. From all these indications, the pathology case 2 should be classified as a solid tendency mass.

The former may be seen as fibrous as well as calcified tissue with relatively high echo content indicated by the energy index Ie. This may indicate a reactive or inflammatory process by the liver. On the other hand, the higher frequency occurrences shown in the power spectrum and the center frequency value in the table 5.5 indicates coarse texture. The prominent peak, shown in the power spectrum as well as the autocorelation graph indicate some periodicity and therefore describing certain regularity and homogeneity in this tissue structure that is most of the time an indicator of solid pattern

The combination function leads to solid mass diagnosis expressed as follows,

$$F_d = F_s \times F_{wr} \hspace{3cm} (5.43)$$

Note that some of results obtained here are in accordance with those obtained in 2-D sample analysis in sect. 4.2 of chapt. 4 .

The clinical significance of the solid-liquid mass differentiation is that, a lesion which is completely cystic has higher probability of being benign than many solid or partially solid which, in many anatomical sites,must be considered as malignant or potentially malignant [1].

To go deeply in differentiating between different pathologies of similar pattern or classes, other feature in the frequential analysis should be taken into account. Besides the center frequency, the bandwidth as well as prominent peaks in the power spectrum could be evaluated and used in decision making for higher probability of success in differentiating between cancer pathologies in the liver.

6- Results
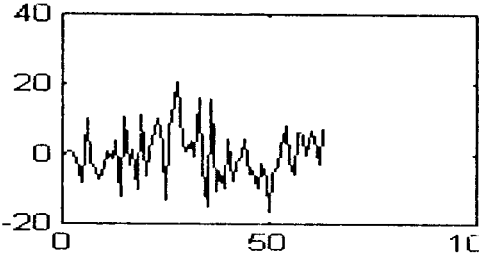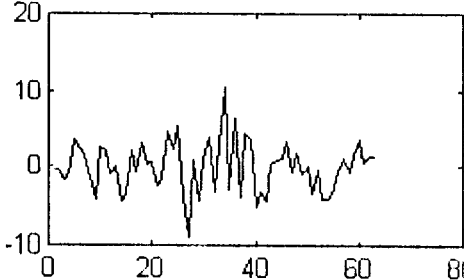
	Cross-Correlation	ρxy
case of study 1		1 -0.0101 -.0101 1
case of study 2		1 -.107 -.107 1

Table 5.1 The cross-Correlation
of a normal trace with the abnormal one

case 1   case 2
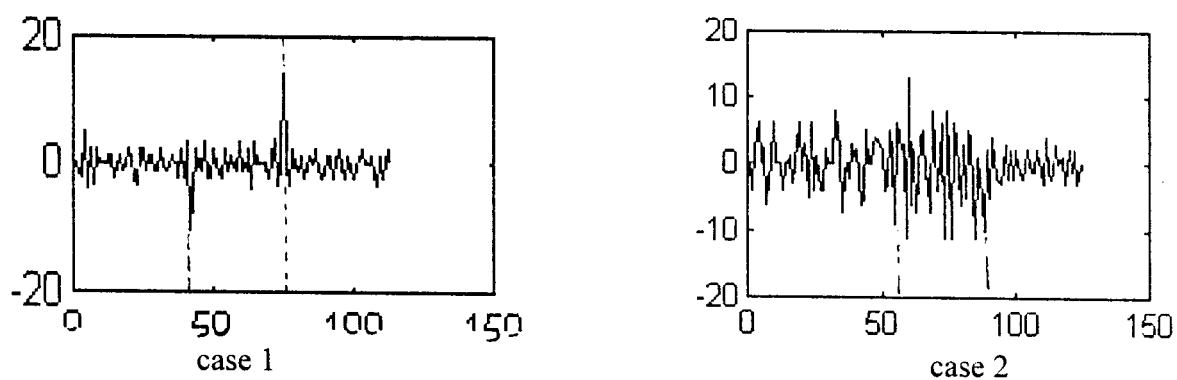
Fig-5.7 Walls detection and location

	Case 1	case 2
AOI images		
A-trace signature A(t)	Reflection A(dB) 20 15 10 5 0 — Normal liver / Lesion / Beyond lesion — 0 20 40 60 80 100 120 X(pix)	A(dB) 20 10 0 -10 — Normal liver / lesion / beyond lesion — 0 50 100 150 X(pix)
Probability density function Pd	N(pix) 10 5 0 — Pathology / Sane liver region — 2.59 10 12.71 20 30 Reflection (db)	N(pix) 10 5 0 — Normal liver / Lesion — 10 13 15 09 30 40 Reflection amplitude(dB)
Walls reflections	A(dB) 20 15 10 5 0 — Af Ab Tw — 0 20 40 60 80 100 120 X(pix)	20 15 10 5 0 — 0 50 100 150

Table 5.2 AOI's, displayed trace signatures and results for cases study 1 & 2

	Peak value (db)			Wall thickness(mm)	
	A_f	A_b	$\Delta R = (A_b - A_f)$	R_w	T_h
case 1	15.5	17	1.5	1.12	1.5
case 2	14.86	4.7	-10.15	.31	3

Table 5.3 Walls peak and thickness values

	Tissues	Statistical reflection Values (db)		Energy Index	Perio dicity		Attenuat .
		Mean (μ_1)	σ^2	Ie	Pn	Sd	α_p
case1	Normal liver	**12.71**	1.95	.053	6	3.2	.5
	Pathology	**2.59**	2.05		7	3.75	**.16**
case2	normal liver	**13**	1.10	1.32	4	2.5	**.5**
	pathology	**14.99**	1.13		8	4.24	**2.31**

Table 5.4 Consistency parameters values

Attenuation

α   (db/cm.MHz)

20

10

5

Solid

Case 2

2

1

.5

Soft tissue

.2

Liver

.1

.05   Case 1

.02

.01   liquid

.001

Water   5   10   13   15   20   R
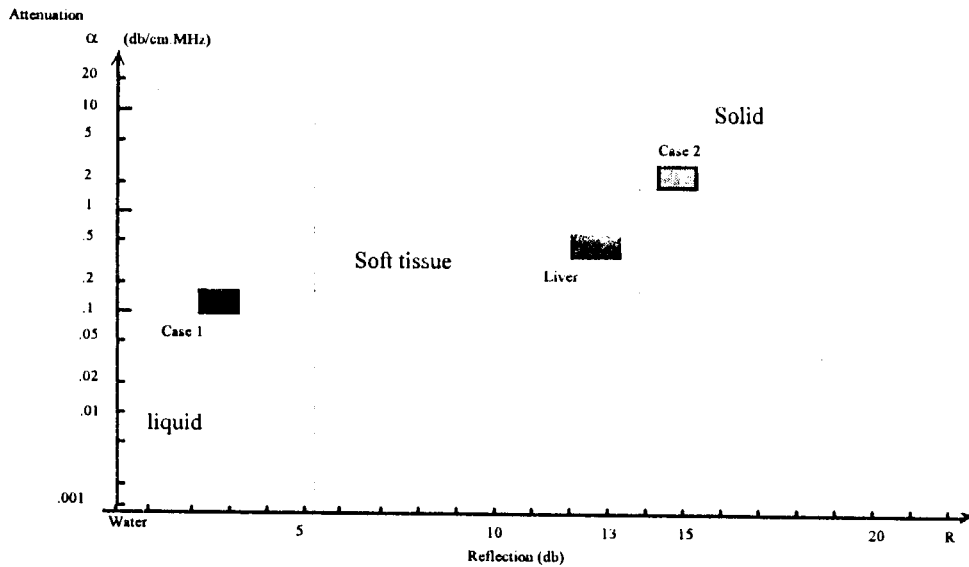
Reflection (db)

Fig-5.8 Consistency classification: attenuation feature versus reflection one

Tissues	Fc (KHz)	Bw (KHz)	Psd	Autocorrelation
Normal liver	245.986	151.203		
case 1	290.611	143.671		
Normal Liver	173.513	111.611		
case 2	319.989	182.078		

Table 5.5 Power spectrum and autocorrelation,

center frequency and rms bandwidth values

CONCLUSION

In this applied research, the work has been directed towards the determination and combination of certain A-mode signal features, that are related not only to the consistency but also to the wall interfaces, which might be characteristic of focal decease's or inclusions.

However, tissue characterization approach, based on the reflection and attenuation parameters estimation, has been used and completed by some evaluated features indicating structural characterization. The obtained results have shown that the envelope detected A-mode analysis has proved to be as efficient as that of RF signal for pathology differentiation. This one-dimensional quantitative approach, in association with image processing, has been applied to two different cases, solid and liquid liver pathologies. They represent respectively benign and malignant cancers, and a good quantitative differentiation has been obtained. But, we are convinced that for a more accurate diagnostic it is required firstly, to perform many tests on a large number of pathological cases and secondly, to use a higher axial resolution in the pulse-echo system to increase the number of data points for the considered small gated portion of the one-dimensional A-trace.

In fact, many difficulties have been encountered, related mainly to :

-Dealing with a relatively new pluridisciplinar biomedical subject where different aspects as acoustic physics, medicine and instrumentation must be understood and linked.

-Collecting reliable acoustic parameters values to constitute data reference and their evolution for the pathological state (cytological data) for a comparison.

-Recording pathological cases at hospitals .

However, the suggested improvements and further work should be oriented mainly to instrumentation and signal processing aspects as:

-The compensation for the non-linearity of the ultrasonic transducer and the electronic system to provide a better acquisition quality of the echo-signal.

-To complete the previous characterization by a dynamic one using Doppler RF frequency shift to sense the tissue motion as well as the blood flow in vascularized regions.

-To exploit the phase change of the echo-signal, besides changes in the amplitude and frequency.

-To use the Wavelet theory, which provides a time-frequency representation, to localize the evolution of frequency with a tissue depth (or time).

-To provide an Automatic A-mode pattern recognition whose classification is based on Bayes decision making.

Finally, the combination of the two techniques image and signal processing, using PC based system, has proved to be fruitful in advancing the state of art in many difficult problems in tissue classification that require analysis from pattern recognition for a non-invasive confirmation of an early stage cancer and therefore, increasing the survival probability of patients.

REFERENCES

[1] Joseph L. Rose and Barry B. Goldberg
Basic Physics in diagnostic ultrasound
Chapt.10 and Chapt. 13 ed. A Wiley Medical publication , 1979.

[2] M.Linzer and S.J.Norton
Current status of ultrasonic tissue characterisation
Seminars in Ultrasounds, Vol. 4 , Mar. 1983 , pp 3-9 .

[3] D.N. White , M.D, General Editor
Recent advances in ultrasound in biomedicine
Chapt. 2, Chapt. 7 , Vol. 1, Research Studies Press, 1977 , pp. 131-135, 152-153.

[4] L.A Geddes & L. E Baker
Principles of applied biomedical instrumentation
Chapt. Application of Ultrasound , Wiley & sons , 1989 , pp. 171 -189

[5] P.N.T Wells
Pulse echo techniques IEEE medical electronic nomograph 23-27
Chapt. Ultrasonic imaging , 1977.

[6] F. Gremy and F. Letterier,
Elements de Biophysique Tome 1
Chapt. 48, Ultrasons , Utilisation en medecine, Flammarion medecine -science ,1981.

[7] P.N.T Wells
IEEE Medical electronics momograghs 1-6
Chapt. Clinical application of ultrasonics, Ed. B. W.Watson, 1971.

[8] D.O .Cosgrove and CR Hill
IEEE medical electronic nomograph 28 -33
Chapt. Ultrasonic imaging of abdomen Ed.B.W. Watson, 1979.

[9] Hua Lee & Glen Wade,
Acoustical Imaging
Plenum press, 1989, pp 1-25 , 345-362.

[10] Ultrasonics International 81
Conference Proceeding
Brighton, UK june 30-july 2, 1981. pp. 222-238

[11] Julius S. Bendat and Allan G. piersol
Engeneering application of correlation and spectral analysis
Chapt. 2, Interscience John Wiley and Sons, 1980.

[12] H.F Polars

Sound wave in the solids

Pion Limited, 1987 , pp.324-334 , 181-183.

[13] Rafael C. Gonzales

Digital image processing

Chapt. 4 , Addison Wesley pulbli. hing company, 1987, pp.19-25.

[14] Zang-Hee cho , Joie P.Jones and Manbir Singh.

Foundations of Medical Imaging

Chapt.14 and 15, Wiley Interscience Publication, John Wiley & Sons, 1993.

[15] Walden A.T

Spatial clustering using simple summaries of seismic data to find the edge of oil field

Applied statistics 43, No.2, 1994 ,pp 385-398.

[16] Fink, M. and Hottier, F.

Short time Fourier analysis and diffraction effect in biological tissue characterization

Acoustic imaging Plenum 12, 1982, pp 493-503.

[17] Stephen P. Banks

Signal processing , Image processing and Pattern recognition

Prentice Hall, 1991, pp. 197-201

[18] James E.CRouch and J. Robert Mc Clintic

Human anatomy and physiology 2nd edition

J. Wiley and Son 1976, pp 617-619

[19] Enders A. Robinson and Sven Treitel

Geophisical signal analysis

Prentice HAll 1980, pp 295-303

[20] George Broun & Claude Moreau

Les Equipement Biomedicaux

Maloine S.A Editeur 1981, pp 91-99, pp 253-271

[21] M. Chafai and H. Bourdoucen

Biological tissue classification and pathology recognition using ultrasonic A-mode signal analysis.

IEEA 97 , International Annual Conference University of Batna, Algeria Dec.97

[22] George Broun & Claude Moreau

Les Equipement Biomedicaux

Maloine S.A Editeur 1981, pp 91-99, pp 253-271

[22] Technical documentation of echographs

Manufact. Pie Data Medical & Toshiba

APPENDICES

-Appendix A : Data extracted fom references [1,4,9]

Parameters	Velocity c m/s	Density ρ	Acoustic impedance Z	Attenuation at 1Mhz/cm	Frequency dependance
Tissues					
Liquid	1520	1.0	1.52	.05	
water(37°)	1480	1.0	1.48	.002	F^2
blood	1570	1.055	1.61	.18	
SoftTissue					
Liver	1540-80	1.06	1.64 -1.68	.94	F
Spleen	1556-78	1.04	1.63		$F^{1.5}$
Kidney	1560	1.04	1.63	1	
Muscle	1538	1.08	1.65 à 1.74	1.5 to 2.5	
Fat	1450	.95	1.38	.63	
Collagen			1.68-- 1.685		
Skin					
S-T average	1540	1.06	1.35 to 1.68	.3 to 1.5	
Solid					
Bone	2700-4100		3.75 -7.38		F to $F^{1.5}$
mass				10.5	
calcified			1.74 -1.78	>45	
fibrous	1504-1537		1.55 -1.70	5.6 -10.1	
cirrhos			1.85 --1.92		
Tumor			1.657	10.5	

Table A.1 Acoustic physical parameters for different tissues and organs

	Air	Water	blood	Fat	liver	spleen	kidney	Muscle	Bone
Water	0.0								
Blood	0.0	28							
Fat	0.0	29	22						
Liver	0.0	25	38	21		40			
Spleen	0.0	22.9	44.2	18	40				
Kidney	0.0	26	44	22	41				
Muscle	0.0	23	31	20	37		32		
collagen									
Bone	0.0	3.3	3.6						

Table A.2 Intensity reflection coefficient values of tissues interfaces.
The corresponding amplitude reflection coefficients are of half values of those indicated in this table.

Parameters	Znw=Z/Zo	Rn= (Znw1/Znw+1)	Rn(db)	Attenuation at 1Mhz/cm
Tissues				
liquid				
Liquid	1.027	.013	-18.75	.025
water(37°)	1	0	-25	.001
blood	1.087	.0416	-13.8	.09
Soft Tissue				
Liver	1.108-1.135	.0512-- .0632	-12.9---11.99	.47
Spleen	1.10	.0476	-13.22	
Kidney	1.10	.0476	-13.22	.5
Muscle	1.11-1.17	.052-- .078	-12.8-- -11.06	.75 to 1.25
Fat	.93			.315
Collagen	1.13--1.138	.061--.064	-12.4---- -11.9	
S-T average				.15 to .75
Solid				
Bone				
mass				5.25
calcified	1.175-1.2	.080-- .09	-10.94---10.41	·22.5
fibrous	1.05-1.15	.024 -- .069	-16.19---11.61	5.6 -10.1
cirrhos	1.25 -1.3	.11 -- .13	-9.5 --- 8.84	
Tumor	1.12	.056	-12.48	5.25

Table A.3 Amplitude reflection and attenuation coefficients values

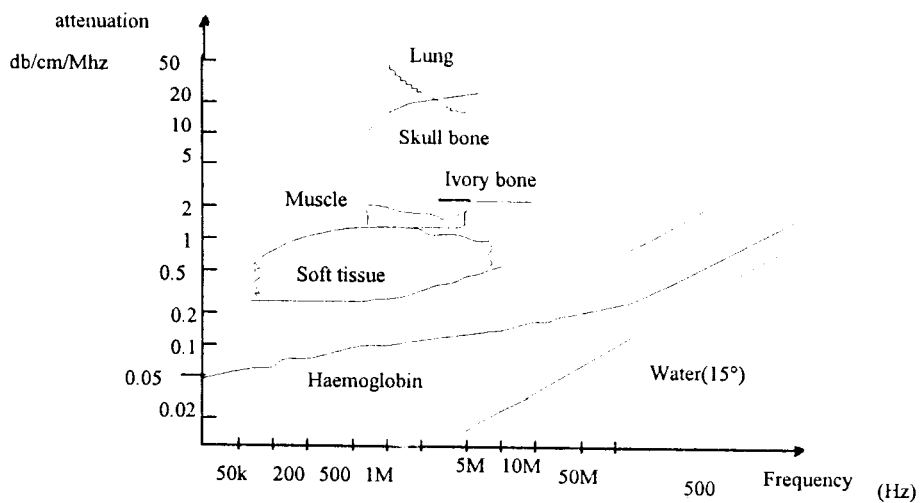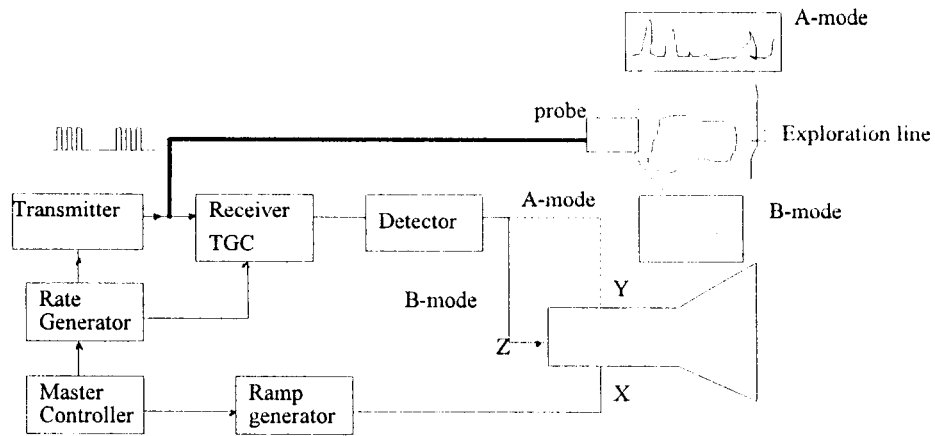Fig-A.4 Attenuation coefficients map of different tissues (From Wells)

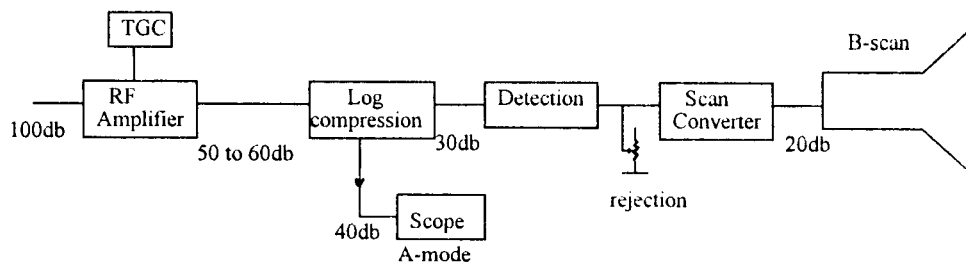Fig-B.1 A and B scans pulse echo system principle
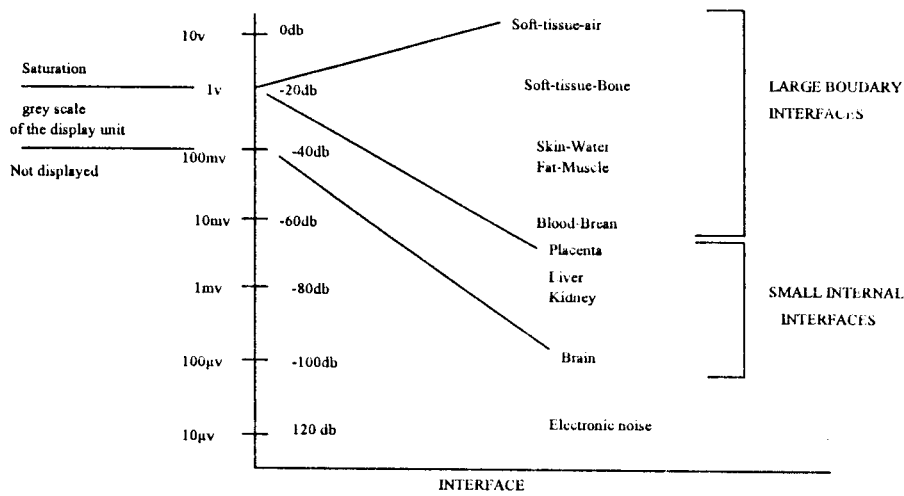

Fig-B.2 Dynamic range of the pulse echo-system

Fig B.3 The dynamic range of the B-scope

The dynamic range of the B-scope is quite small (around 20db) this is much less than that of the A-scope display which may have a dynamic range of around 40 db. So a mode A presents more clinical information w.r to B-mode.Then the A-signal can be taken off naturally, after the detection to be displayed on the scope.

-Characteristics of the used echograph:

  -Linear probe composed of 64 transducers (transmission per group of 8)

  -working at frequency : 3.5Mhz   (axial resolution =.44mm)

  -gray level resolution : 64 (corresponding to 36db)

  -Nbre of vertical A mode lines: 128

  -Screen matrice: 256x256 pixels (interlacing system)

  -video output
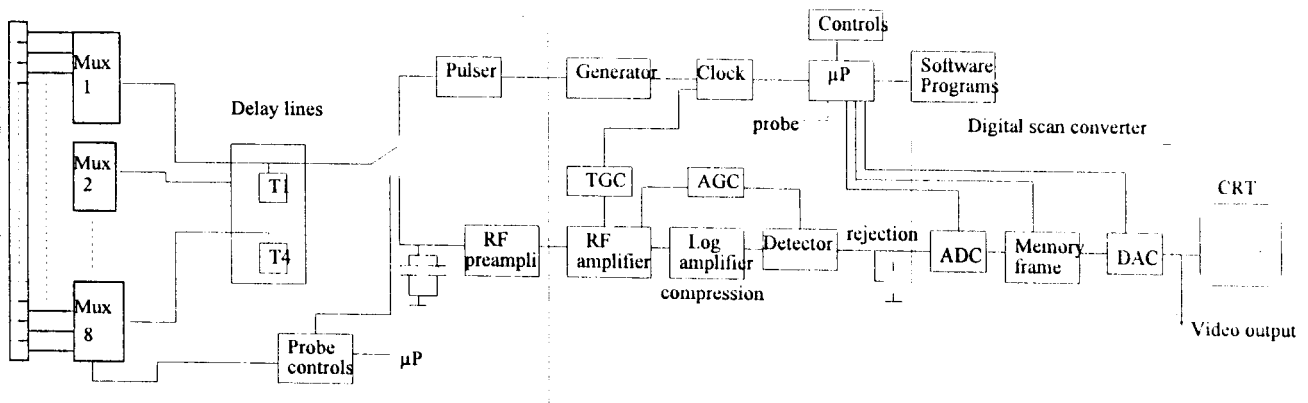
  -PRF >4000/s

  -Transmited ultrasonic intensity : 10mw

Fig-B.4 Detailed block diagram of the used echograph [21]

-Characteristics of the acquisition video card Pixel view

  -Full motion video prteview in windows environmemt at 15 frames/s

  -True color frame capture : Size: -640x480 for NTSC

                                       -768x576 for PAL

  -Resolution (color or grey scale): 8-16 and 24 bits per pixel

  -Cropping to get AOI down to 40X30 pixels
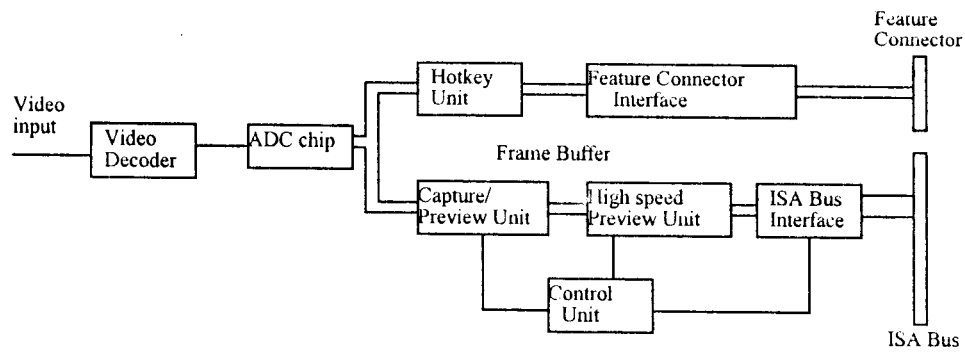
  - parametrable

  -Full screen video hot key

Fig - B.5 Functional block diagram of Pixel view acquisition card

		RMS	Range	Skewness
case1	Normal liver	1.39	5	-0.60
	Pathology	1.43	6	-0.85
case2	normal liver	1.14	4.25	.34
	pathology	1.1.08	3.86	.52

Table C.1 Other statistical valuesfor pathology cases 1 and 2

.Pathology	Probability
Liquid L	60%
Solid S	30%
Mixed SL	10%

Table C.2 Probabilities existing upon examination of patients over peroiod of time[1]

| Pathologies | Consistency | | | | | | | | Walls | | | | Fd |
| | R | | | α | | | Sd | | Th | | Pk | | |
	R_L	R_m	R_s	α_L	α_m	α_s	S_{d1}	S_{d2}	T_{h1}	T_{h2}	P_{k1}	P_{k2}	
Cyst	*			*			*		*		*		$(R_L\,\alpha_L\,S_{d1}T_{h1}P_{k1})$
Hemangiom	*				*				*		*		$(R_L\,\alpha_m T_{h1}P_{k1})$
Biliary Cyst	*			*					*				$(R_L\,\alpha_L\,T_{h1})$
Hematoma Ascites	*			*			*			*			$(R_L\alpha_L S_{d1}T_{h2})$
Solid mass			*		*			*		*		*	$(R_s\alpha_s S_{d2}T_{h2}P_{k2})$
Cirrhos			*		*					*			$(R_s\alpha_s S_{d2}T_{h2})$
Metastas			*		*								$(R_s\alpha_s)$
Mixed L-S		*											$(R_m\alpha_m)$

Table C.3 Classification of pathologies obtained by the combination of
the consistency and walls parameters

	RADIOLOGY	ECHOGRAPHY	GAMMA Camera	NMR
Price	100 KF to7.8MF	100KF to 1MF	2MF	6 to 13MF
Resolution		Axial< 1mm	2 ou 3mm	x .1mm
Inocuity	** to ***	none	** to ***	0 to *
Gray scale		>64	>64	>64
application	Anatomy	Anatomy	Functionnal	Anatomy

Fig-1 Comparison table
Cost-quality with respect to other imaging systems
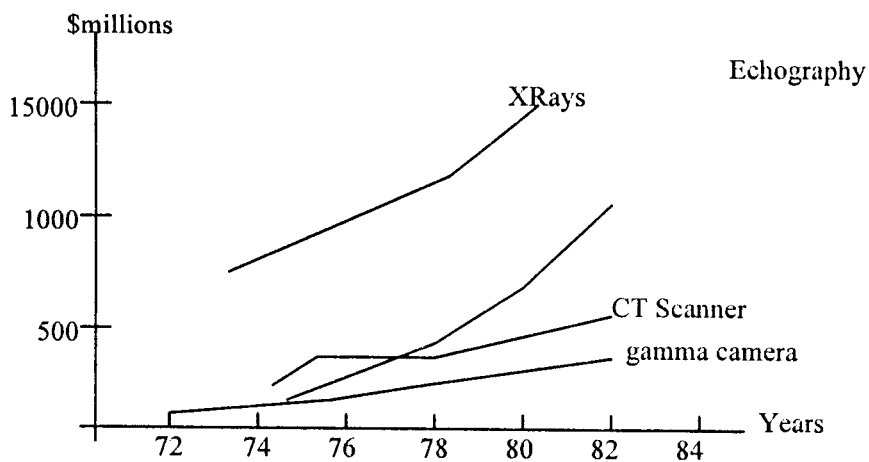

Fig-2   Evolution of the market in imaging systems

Appendix E

Biological tissue classification and pathology recognition using ultrasonic A-mode signal analysis.

M. Chafai and H. Bourdoucen
Institut National d'Electricite et Electronique
INELEC CP 35000 Boumerdes, Algerie Fax :02-821400

Abstract

In this work , B-scan echographic images, obtained from the video output of an echograph using an ultrasonic linear probe, are recorded on a VCR. The recorded still images are introduced into a PC via a video acquisition card to be captured and optimally processed in order to outline the areas of interest (AOI's) . The selected AOI is converted to gray level matrix and individual column vectors , representing the one-dimensionnal A-mode lines, are extracted and then analysed on the base of their amplitude weights for tissue classification and pathology recognition .

Keywords: characterisation, ultrasounds, A-mode, reflection, attenuation, quantitaive,tissue,pathology

1-Introduction

The subject of tissue characterisation using ultrasounds is receiving much more attention nowadays by biomedical engineers community. Most of the investigations published in the litterature within the last two decades, from the quantitative approach point of view, are oriented, in majority, to the tissue consistency determination. In connection to this approach, the statistical and the FFT analysis of the corresponding RF A-mode signal are particularly the mostly used tools [1].

In this work , the A-mode trace is obtained from the envelope detected echo signal which is then, gated into several portions to end up with traces of interest corresponding not only to the consistency, but also to the boundary feature. This last feature is also important clinically, since it is indicative of the focal decease in the liver[1]. These two clinical features are expressed in terms of A-mode signal parameters whose combination is used firstly, for tissue classification (liquid-solid) and secondly, to characterize the focal pathology for early-warning cancer detection.

2- Interaction of ultrasounds with biological tissues

The simultaneous existence of so many different and complex interactions of ultrasounds with biological tissues and their dependence on temperature makes difficult to isolate anyone of them with a high degree of accuracy. Some necessary simplifying assumptions are made regarding the other interactions that can affect the pulse-echo signal and only backscattering behaviour is observed in imaging device when taking into account the attenuation estimation for tissue characterisation [2].

Fields and Dunn (1983) [3], considered the classical formula for the amplitude coefficient of backscatterer R as:

$$R = \frac{Z_2 - Z_1}{Z_1 + Z_1} \qquad (1)$$

where Z_1 and Z_2 are respectively, the charactetristic acoustic impedances for two adjacent tissues .

The reflected amplitude Ar is directly proportionnal to the reflection coefficient R as:

$$A_r = A_i . R \qquad (2)$$

Where A_i is the incident amplitude or pressure.

For further convenience, the specific acoustic impedance is normalised with respect to that of the water Z_0 .

In this study, we have considered only the first order reflections with planar interfaces, in which the ultrasound beam can either be specularly reflected or backscattered with taking into count the progressive attenuation of the beam (see Fig .1). In the case of n layers to be traversed by an ultrasound beam, the detected reflected amplitude at the Kth interface can be expressed as follows :

$$Ar_{k,k+1} = \begin{cases} A_i R_{12} & \text{for } k = 1 \\ A_i \left(\prod_{p=2}^{p=k} \left(1 - R_{p-1,p}^2\right) \right) \exp(-2 \sum_{m=1}^{m=k-1} \alpha_m x_m) . R_{k,k+1} & \text{elsewhere} \end{cases} \qquad (3)$$
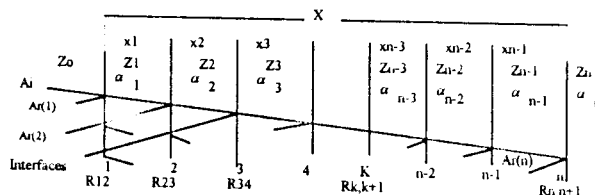

Fig. 1- Reflections at different interfaces of an n-layer tissue

Where n is the number of interfaces and Z_k, α_k and x_k are respectively, the specific acoustic impedance, the attenuation coefficient and the thickness of the Kth layer. This signal should be applied to a time gain compensation circuit (TGC) in the pulse echo system to compensate for the attenuation. The TGC function is generally taken as an increasing exponentiel time function $(\exp(\alpha c.t))[1]$

For the estimation of the attenuation in reflection mode we have considered the reflection amplitude reduction at the kth interface which is evaluated as the diffrence between the reflection amplitudes of the front wall A_{R12} and the back walls $Ar_{k,k+1}$. Assuming that both walls have the same backscattering coefficient $A_{ik,k+1}$, the

attenuation coefficient of the considered medium at the working frequency f per cm is estimated as follows:

$$\alpha \cong \alpha_c - \frac{(A_{r,i,1} - A_{r,i2}) - \sum_{p=2}^{p=K} Log(1 - R^2_{p,p,1})}{X.F} \qquad (4)$$

Where α_c , X , F and P are respectively the set TGC coefficient, the tissue thickness, the working frequency and the periodicity.

3-The PC based pulse-echo system

The pulse-echo system, we have used, consists essentially of an ultrasoinc linear array probe (pulser-detector), a receiver and a scan-converter with a microcontroller. The probe is made of an array of *64* fixed transducers placed in a linear configuration and providing *120* A-scan lines which will built up, in real time, a B-scan image [4].
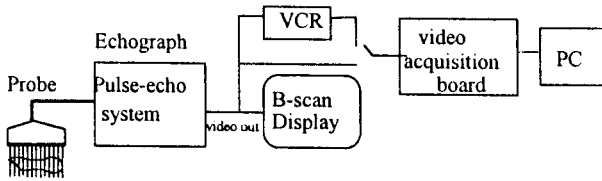

FIG . 2 PC-based pulse-echo system

The recorded B-scan echographic images are introduced into a PC via a video acquisition card to be captured and optimally processed in order to outline the area of interest (AOI). This AOI should include the normal and the abnormal regions of the liver and the region beyond the lesion. Individual column vectors Of this AOI, representing the A-mode lines, are extracted and analysed on the base of their amplitude weights for tissue classification and pathology recognition .

4- Pathology detection

When excited by a high voltage pulse, the ultrasonic transducer produces a wavelet that will be transmitted into the human tissue that is composed of a series of n intefaces acting as reflectors [3](refer to Fig. 3).
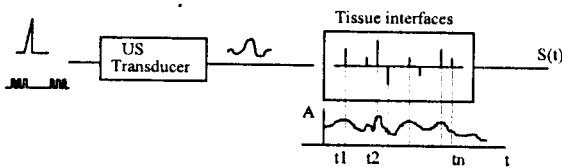

FIG 3 System modeling for A-mode signal tissue reflection

The transducer will receive, from these reflectors, a series of impulse response at times ti and the overall response produces a trace S(t) that is expressed as :

$$S(t) = \sum_{i=1}^{n} Ri.w(t - t_i) \qquad (6)$$

where R_i and, $w(t-t_i)$ are respectively ,the reflection coefficient and the weight of the wavelet at the ith reflector.

the present pulse echo systems are based on the envelope detection method and therefor a low pass filter is used to suppress the carrier frequency and the HF noise to end up with an envelop that is the monodimensional A-mode trace given as follows:

$$A(t) = S(t).H_{pe} \qquad (7)$$

Hpe is the pulse echo system transfer function.

The consideration of different regions of the same organ , with the normale one taken as the local reference, as well as the use of the same ultrasonic beam path should allow an efficient tissue differentiation. The processing operations such as normalisation, gating the normal and abnormal traces of interest (TOI) and their correlation are performed preliminary.

For the consistency fine selection, the time gate (t2-t1) within the range of 13 to 26μs , corresponding to a time of flight of 1 to 2 cm, is suitable for echo video signal analysis for early detection of cancer[7].

On the other hand, the A-mode signal pattern recognition skills play an important role in arriving at reliable diagnosis of inclusions or focal deceases using most of the time both the boundary and the consistency features.

These two last parameters, which are indicative of the pathology, are expressed in terms of the signal parameter [5] such as amplitude averages , peak values, frequency content,etc.. .These two clinical recognition features are used first for tissue classification, liquid-solid-mixed, and then for characterizing the pathology (malignant or benign) .

4.1-Walls Analysis

The peak value, the thickness and the nature of the back and front walls may identify the type of pathology. This applies most of the time to focal deceases such as cyst which has a smooth wall or a solid decease as hematoma which has a rough one[6].

The wall of the pathology may be located as a positive or negative reflected level transition(s) which depends on the its acoustic impedance relative to the normal liver medium.

This detection is obtained by a differentiation operation or gradient method which assumes relatively large values for rapide transition in the A-mode signal.

. The evaluation of the relative higher peak values reflected at a particular point or laps of time [t1 t2], is efficiently used for an initial profil comparison and further tissue classification. Hence the peak values of the gated signal portion, corresponding to the front or back wall , is evaluated as follows :

$$A_{wp} = Max (A(t)) \qquad for \qquad t1 < t < t2 \qquad (8)$$

The echo strength of a distal wall may be used to characterise the wall nature on the base of the acoustic impedance relative to that of the normal liver.The strenght ratio of the back to front walls peak values, A_b and A_f , can identify the type of the pathology by estimation of the attenuation relative to the normal liver data. That is;

$$R_w = A_b / A_f \qquad (9)$$

For example , in the case where $R_w \ll 1$ there is a lower reflection amplitude producing an acoustic shadow, and hence, the lesion presents a higher attenuation than the normal liver.

The wall thickness parameter is also important in differentiating between pathologies and is expressed as the product of time duration and the ultrasonic speed C as:

$$T_w = (T_h - T_l).C \qquad (10)$$

where T_l and T_h are respectivly the 6db lower and higher time wall limits found by solving :

$$A = 1/2.Max(A_w) \qquad (11)$$

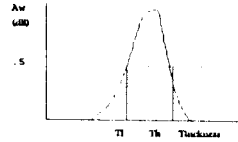**Fig. 4 - Wall thickness**

For instance :

The case $T_w < 3mm$ corresponds to a cystic wall .

The case $T_w > 3mm$ corresponds to a solid mass wall.

In the other hand, a larger wall may be seen as a wall a consisting of line segments called edgels, having a magnitude and a direction. These edgels correspond to discontinuities in the displayed intensity and the corresponding function, that is of nth order , has a delta function with its nth derivative expressed as:

$$\frac{d^n A}{d t^n} = \delta \qquad (12)$$

The Pathology Size X is evaluated as the distance separating the back to front walls. It may be also used for evaluation of the overall attenuation for the lesion and its spatial distibution.

4.2-Consistency Analysis

Among the signal features of high confidence that are used to characterize the consistency, we may quote :

-The reflection amplitude mean (obtained from the probability density function) and the reflection energy .

- The periodicity or the spatial distribution .

-The estimated attenuation

-The frequency contents

4.2.1-Reflection amplitude analysis:

The internal architecture of the tissue is stochastic in terms of acoustic scattering properties then, any change in acoustic impedance is expected to occur randomly. But in the case of the liver tissue which may be considered as homogneous medium, the obtained traces could be deterministic with some degree of ramdomness due to some abnormal phenomenon or pathologies.

Although this effect, an accurate statistical determination of the averages for the A-trace, enables a quantitative

characterisation of a particular biological tissue. This is bestly characterised by its probabilty density function and the averaging measurements.

The histogram $H(G_i)$ of a displayed column vector A is a graph which gives the number of pixels of the same value in each gray class G_i where $0 < G_i < 64$. It is obtained by summing up a number of pixels as:

$$N = \sum_{i=0}^{i=63} H(Gi) \qquad (13)$$

To obtain a graph of the probability density function P(A), the histogram is first converted to a bar chart and then, a curve fitting process is carried out. The various statistical descriptive measures of the A-trace are given by the nth moments [11] that are defined as:

$$\mu_\kappa = E[A^\kappa(t)] = \sum A^k P \qquad (14)$$

This process is limited to the second order ; that is, the reflection mean and the variance .

The first moment, which is the reflection amplitude mean, describes how the reflection process behaves on the average, and it is given by the following sum:

$$\mu_1 = E[A(t)] = \sum A.P \qquad (15)$$

The mean μ_1 ,that is also the measure of the central tendancy, is evaluated ,in db, by statistics as:

$$\mu_1 = \frac{1}{N} \sum_{i=1}^{N} A_i \qquad (16)$$

The variance, that is the second moment, is the measure of the variability or the deviation from the reflection mean.The sampled variance is given by:

$$\sigma = \frac{1}{N} \sum_{1}^{v} (A_i - \mu)^2 \qquad (17)$$

The reflection amplitude varies considerably with time and a convenient representation that reflects these amplitude variations is the short time energy. The measured total amount of the sonic energy(that is the area sustended by the trace) received by the system[10] is evaluated as the sum of the square of its amplitudes Ai , is given by:

$$E_n = \sum_{i=0}^{N} [A_i]^2 \qquad (18)$$

The comparison index Ie is evaluated as to be ratio of the detected anormal energy Ep to the normal (or reference) energy Er that is given:

$$I_{en} = \frac{E_{np}}{E_{nr}} \qquad (19)$$

The periodicity evaluation method is achieved by preselecting an echo amplitude level and determining the number of times the trace crosses such level. This is defined as the number of cycles present in the trace for a given time window T_w .

A zero or a level crossing takes place if the measured samples have different algebraic signs. Thus, the rate at

which this level crossing occurs is the periodicity P_n of the A-trace that can be evaluated as follows :

$$P_n = \frac{1}{2}\sum_{n=0}^{+\infty}|sign[A(m)] - sign[A(m-1)]| \qquad (20)$$

where $sign[A(m)] = 1$ for $A(m) \geq 0$

and $sign[A(m)] = -1$ for $A(m) < 0$

Thie spatial distribution S_d is derived as the ratio the number of periods to the pathology size X and is given by :

$$S_d = \frac{P_n}{X} \qquad (21)$$

Since the working frequency f=3.5Mhz and the set attenuation coefficient of the liver αc is about .5db/cm.Mhz, the attenuation α_p in the case of a consistency without internal interfaces is estimated using (11) as :

$$\alpha_p = \alpha_c - \frac{A_{R2} - A_{R1}}{FX} = 0.5 - \frac{A_b - A_f}{3.5X} \qquad (22)$$

In the case of consistency with some interfaces of the same type and whose number may be approximately equal to the periodicity value Pn, the attenuation α_p is evaluated as follows:

$$\alpha_p = 0.5 - \frac{(A_b - A_f)}{3.5. X} + \frac{P_n . Log(1 - R^2)}{3.5. X} \qquad (23)$$

4.2.2-Reflection spectral Analysis

The frequency profile is often used as frequency signature for characterizing various materials and structures.. It appears of significant values for tissue classification because it has the ability to make distinction between biological phenomena and sources whose frequencies are very close to each other and it is closely related to the measurable quantities.
The N-Discrete Fourrier Transform is given by :

$$X(i+1) = \sum_{k=0}^{N-1} A_{k+1} \exp(-2\pi j(ik/N)) \qquad (24)$$

For i=0,....,N-1

The power spectral density P(f) of a signal is measure of the signal energy at differents frequenies and it is given:

$$P(f) = \frac{1}{n}|X|^2 = \frac{1}{n}XX^* \qquad (25)$$

The measured center frequency Fc is estimated as the average of the square of the FFT[10] given by:

$$F_c = Mean((FFT)^2) = \frac{\sum_{k=0}^{(N/2)-1} P_k F_k}{\sum_{k=0}^{(N/2)-1} P_k} = \frac{\sum_{k=0}^{(N/2)-1} P_k K\left(\frac{f_s}{N}\right)}{\sum_{k=0}^{(N/2)-1} P_k} \qquad (26)$$

where P_k is the power spectrum and fs is the sampling frequency. The RMS bandwidth Bw ,that is estimated as

the variance of the FFT, could be also used for differentiation .

4-Classification and interpretation

The combination of signal features is used for tissue classification (liquid-solid) and then characterizing the pathology (malignant or benign).A combinational tree diagram has been elaborated for the final diagnostic decision (Fig.-4-) below.
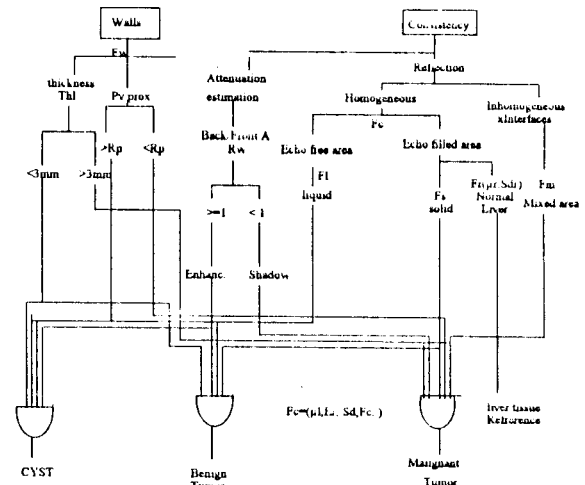

Fig .4 Combinational classification tree diagram.

Since our first objective is to differentiate between liquid and solid masses, two corresponding AOIs , have been considered. Data have been obtained from mathematical analysis that has been presented in previous sections.

-Interpretation :
-Pathology Case1:
The small value of the reflection mean $(\mu_1 = 2.59\ dB)$ ranges within the values which correspond to a liquid class according to Table I (Pd1) ,Fig.5 and Fig-2 of the appendix . However, the small variations in the curve of the trace, due to some spurious echoes, will give a meaningless periodicity. Furthermore, the value of ΔR , which is positive in this case, estimates the value for the attenuation α_p to be lower than that of the liver and it tends to be in the range of that of a liquid. The estimated values for the parameters μ_1 and α_p , which are of highconfidence , will classify this consistency as a liquid. On the other hand, the value of the wall thickness
Tw which is less than 3mm, indicates the presence of a smooth boundary, whereas, the higher value for the reflected peak of the front wall shows a calcified wall [7]. therefore , it is deduced that this pathology is a cyst.
-Patholgy case 2:
The regularity of the trace in case 2 shown in Fig.5- indicates that this pathology is homogeneous. The average value of the reflected amplitude, that is, two more dB's greater than that of a normal tissue, indicates a relatively higher acoustic impedance which corresponds to a solid consistency according to Table I (Psd),Fig.5 and Fig-2 of appendix . Also, the higher value of the periodicity in table 2, shows the presence of multiple echoes or interfaces. The amplitude of the back wall echo is much

smaller than that of the front wall indicating a higher attenuation. In addition to this, we can notice from the previous tables that the walls' thickness ranges critically at *3mm* indicating that their nature is more or less rough . From all these indications, the pathology case 2 should be classified as a solid mass.

The former may be seen as fibrous as well as calcified tissue with relatively high echo content indicated by the energy index Ie. the higher frequency occurences shown in the power spectrum and center frequency value indicates grossiary texture.

The clinical significance of the solid-liquid mass differentiation is that,a lesion which is completeley cystic has higher probability of being benign than many solid or partially solid which, in many anatomical sites, must be considered as malignant or potentially malignant [1].

5-Conclusion

This quantitative approach presented in this paper, has been applied to two different cases, solid and liquid liver pathologies. They represent respectively benign and malignant cancers, and a good quantitative differentiation has been obtained on the base of the high confidence signal indicators. But, we are convinced that for a more

accurate diagnostic it is required firstly, to perform many tests on a large number of pathological cases and secondly, use a higher axial resolution to increase the number of data points for the considered small gated portion of the A-trace.

	Af (db)	Ab	Rw	Ab-Af	T_w(mm)
case 1	15.5	17	1.13	1.5	1.5
case 2	15.06	4.91	.3	-9.97	3

Table I Walls peak values

	Tissue	$\mu_{1\,db}$	σ	E Kj	Ien	Pn	α_p	FcKhz
case1	Normal liver	12.71	1.93	5.237	.053	6	.5	245.98
	Pathology	2.59	2.04	.279		7	.21	290.6
case2	normal liver	13	1.29	5.44	1.32	7	.5	173.51
	pathology	15.09	1.14	7.18		9	2.31	319.98

Table II consistency reflection values

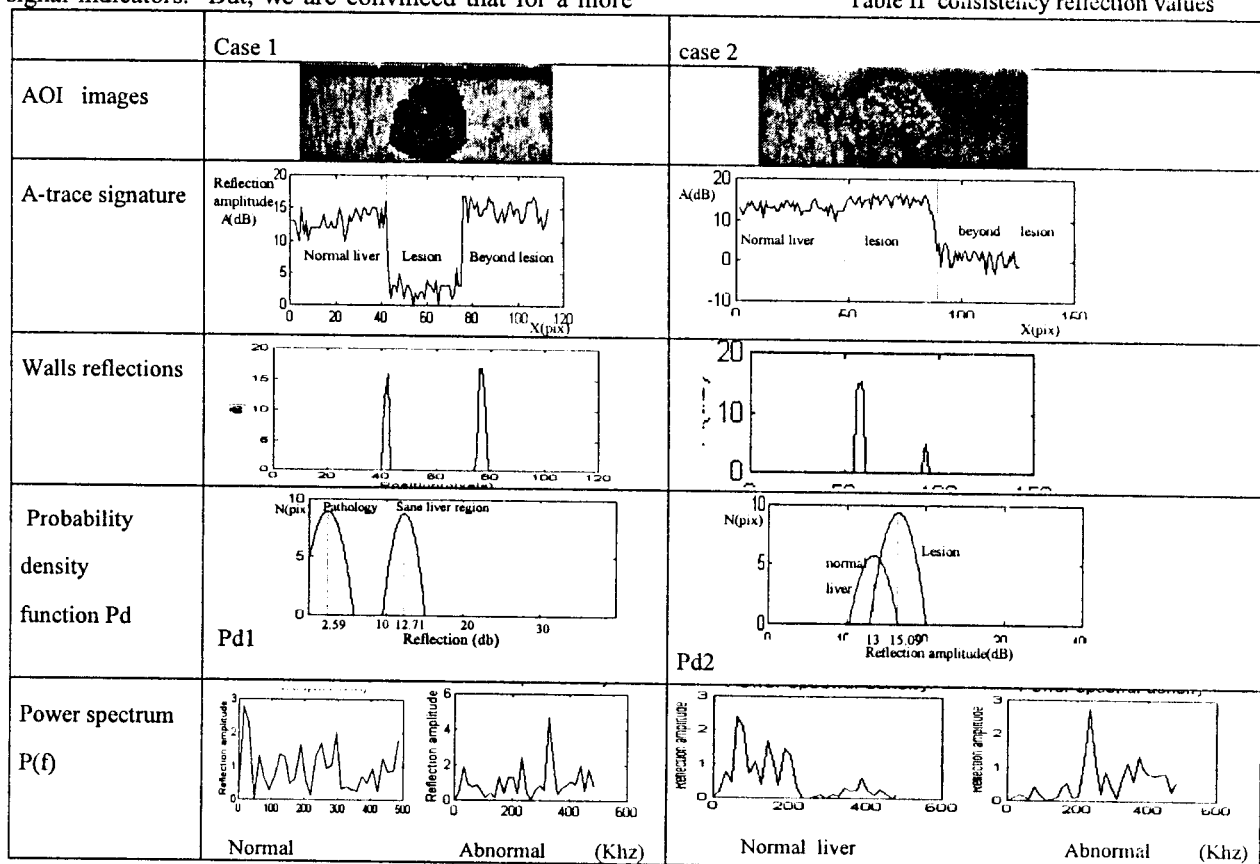|	Case 1	case 2
AOI images		
A-trace signature		
Walls reflections		
Probability density function Pd		
Power spectrum P(f)		

FIG-5 AOI's ,displayed trace signatures and graphical results for cases study 1 & 2

Appendix

Data fom [1,4,9]
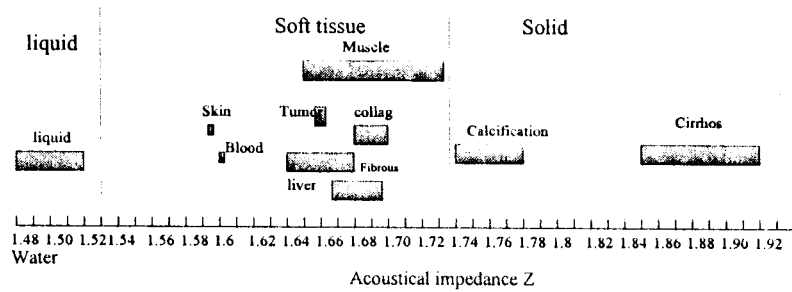
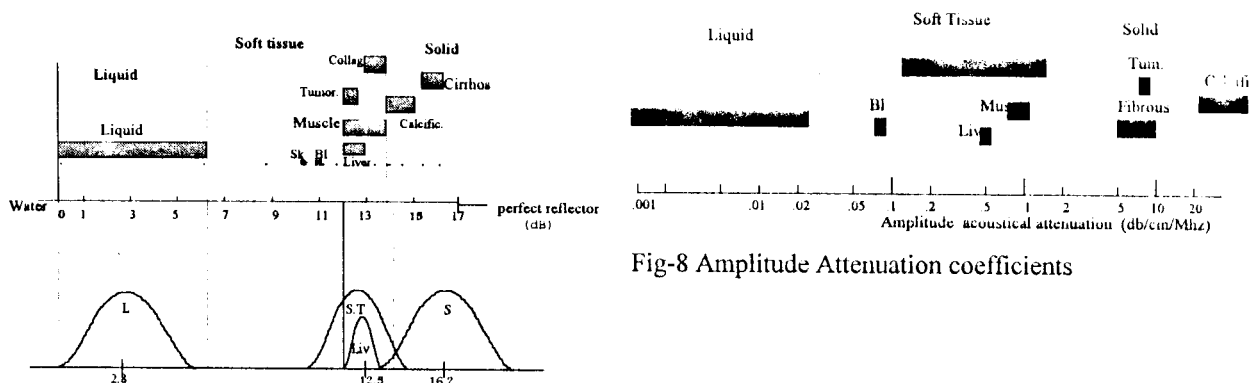Fig-6 Acoustical impedance scale (Kg s^{-1} m^{-2})

Fig.7 Reflection amplitude classes and distribution

Fig-8 Amplitude Attenuation coefficients

References:

[1]Joseph L. Rose & Barry B. Goldberg "Basic Physics in diagnostic ultrasound ",Chapt 10, Chapt 13 ed. A Wiley Medical publication 1979

[2]M.Linzer &S.J.Norton "Current status of ultrasonic tissue characterisation " Seminars in Ultrasound, Vol. 4 pp 3-9 ,mars,1983

[3] D.N. White ,M.D,General Editor " Recent Advances in ultrasound in biomedicine " chapt 2 , Chapt 7 , pp. 131-135, 152-153,Volume 1, Ed. RSP 1977.

[4] L.A Geddes & L. E Baker Principles of applied biomedical instrumentation chapt . Application of Ultrasound pp. 171 -189 Ed. Wiley & sons Inc, New-york ,1989

[5] P.N.T Wells IEEE medical electronic nomograph 23-27 ,Ultrasonic imaging , Pulse echo techniques ,1977

[6] F.Gremy et F Letterier , Elements de Biophysique Tome 1 chapt. 48, Ultrasons : utilisation en medecine Ed. Flammarion medecine - science ,1981.

[7]P.N.T WELLS IEEE medical electronics momograghs 1-6 Clinical application of ultrasonics pp. 146- 180 Ed.B.W Watson, 1971

[8] D.O .Cosgrove and CR Hill , IEEE medical electronic nomograph 28 -33,Chapt.US imaging of abdomen Ed.B.W Watson,1979.

[9] Hua Lee & Glen Wade, Acoustical imaging , Ed. Plenum press 1989.

[10] Ultrasonics International 81, Conference proceding Brighton,UK 30 june-2july 1981 p-p 222-234

[11]Julius S. bendat and Allan G. piersol ,Engeneering application of correlation and spectral analysiswiley ,chapt 2 Intersicience J.Wiley & Sons 1980.